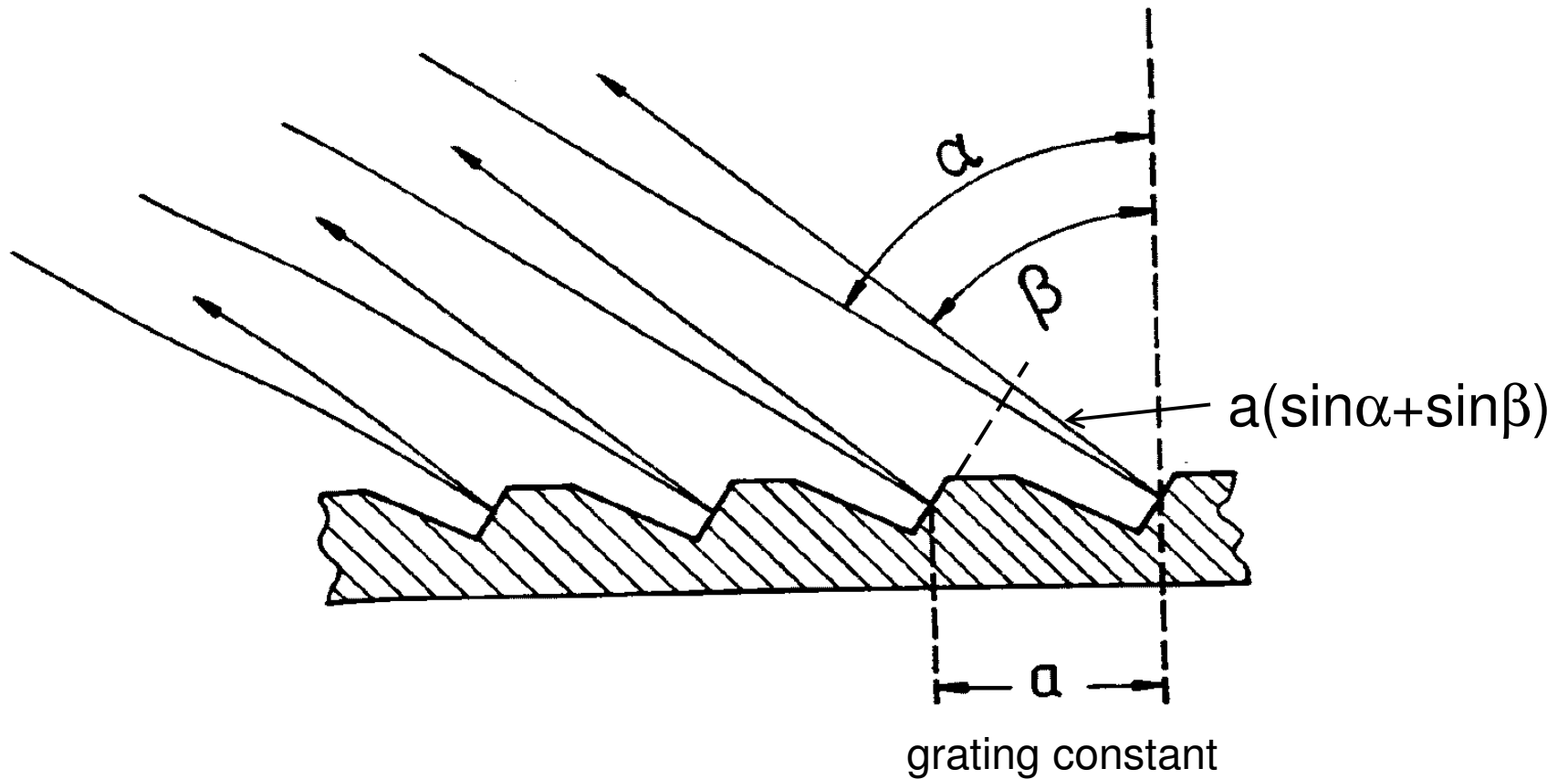


## **4. Tools for Solar Observations-II**

Spectrographs. Measurements of the line shift.

# Spectrograph

Most solar spectrographs use reflection gratings.



**Blazed reflection grating (echelle grating).**

Consider a reflection grating with a distance between grooves,  $a$ , ('grating constant'). If  $\alpha$  is an angle of incidence, and  $\beta(\lambda)$  the angle of diffraction, then the directions of the maximum intensity,  $\beta$ , are given by the 'grating equation':

$$m\lambda = a(\sin \alpha + \sin \beta),$$

where  $m$  is the order of the spectrum. Differentiation of this equation gives the angular dispersion:

$$\frac{d\beta}{d\lambda} = \frac{m}{a \cos \beta}.$$

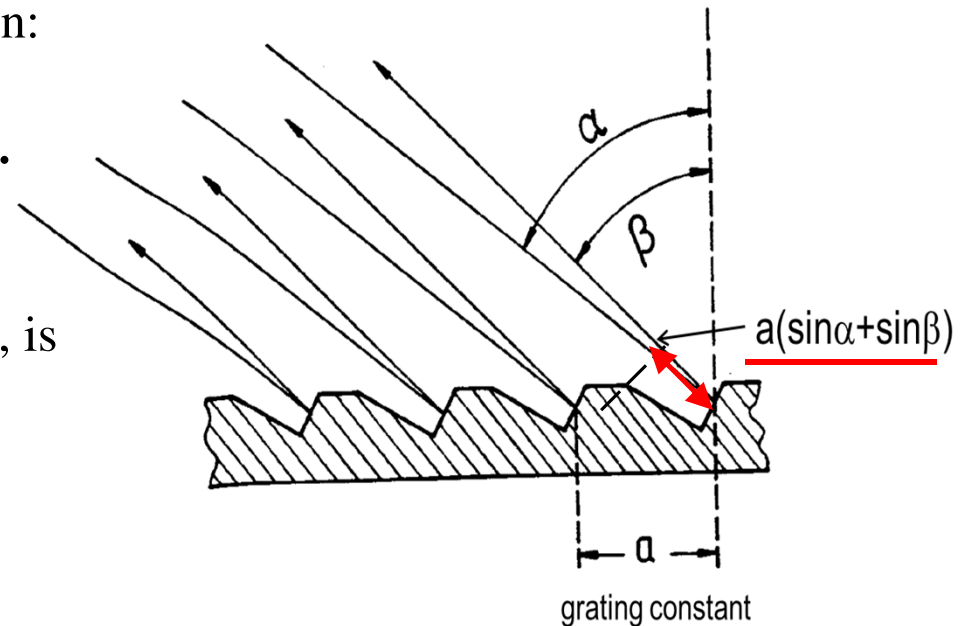
The linear dispersion in the focal plane,  $f$ , is

$$\frac{dx}{d\lambda} = f \frac{d\beta}{d\lambda}.$$

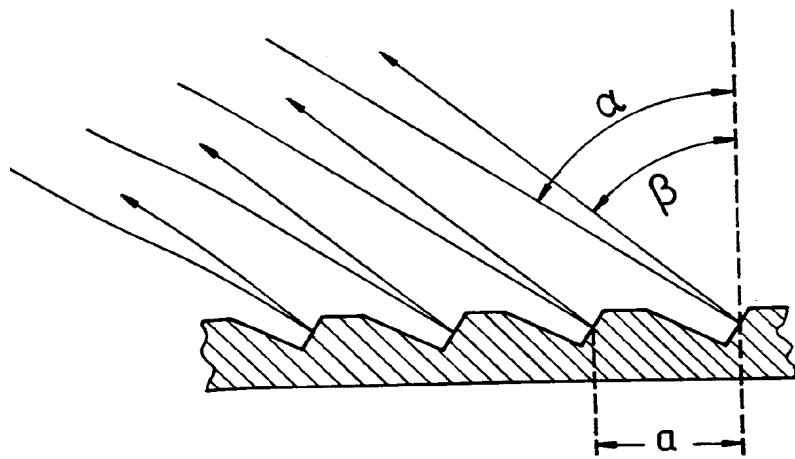
For  $\beta \approx \alpha$ ,

$$f = \frac{dx}{d\lambda} \frac{a \cos \alpha}{m}.$$

A typical grating has 600 grooves/mm, and typically,  $m = 5$ ,  $\alpha = 60^\circ$ . If we want to have a resolution  $dx/d\lambda = 6 \text{ mm}/\text{\AA}$ , then the focal length,  $f \approx 9.5 \text{ m}$ .

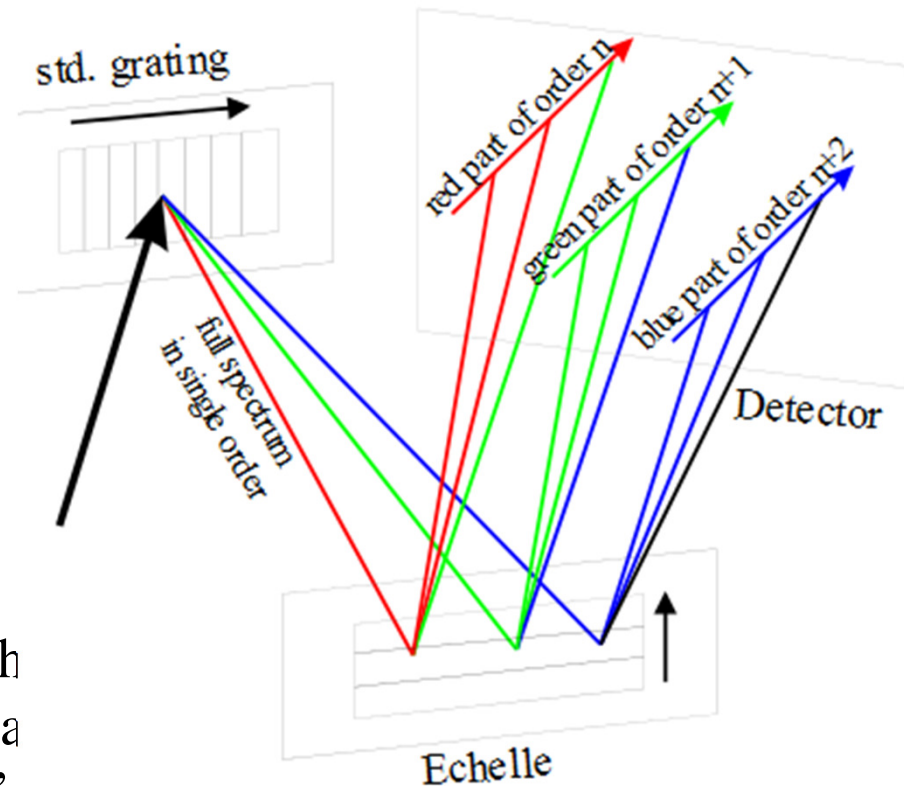


# Echelle grating



Echelle gratings allow to work with high orders  $m \approx 50$ . They have a special profile, strongly 'blazed', and have high reflectivity. The spectra for various order  $m$  may overlap, and this is used to record simultaneously several lines with a single camera. Unwanted parts are separated by masks and filters.

# Echelle spectrometer

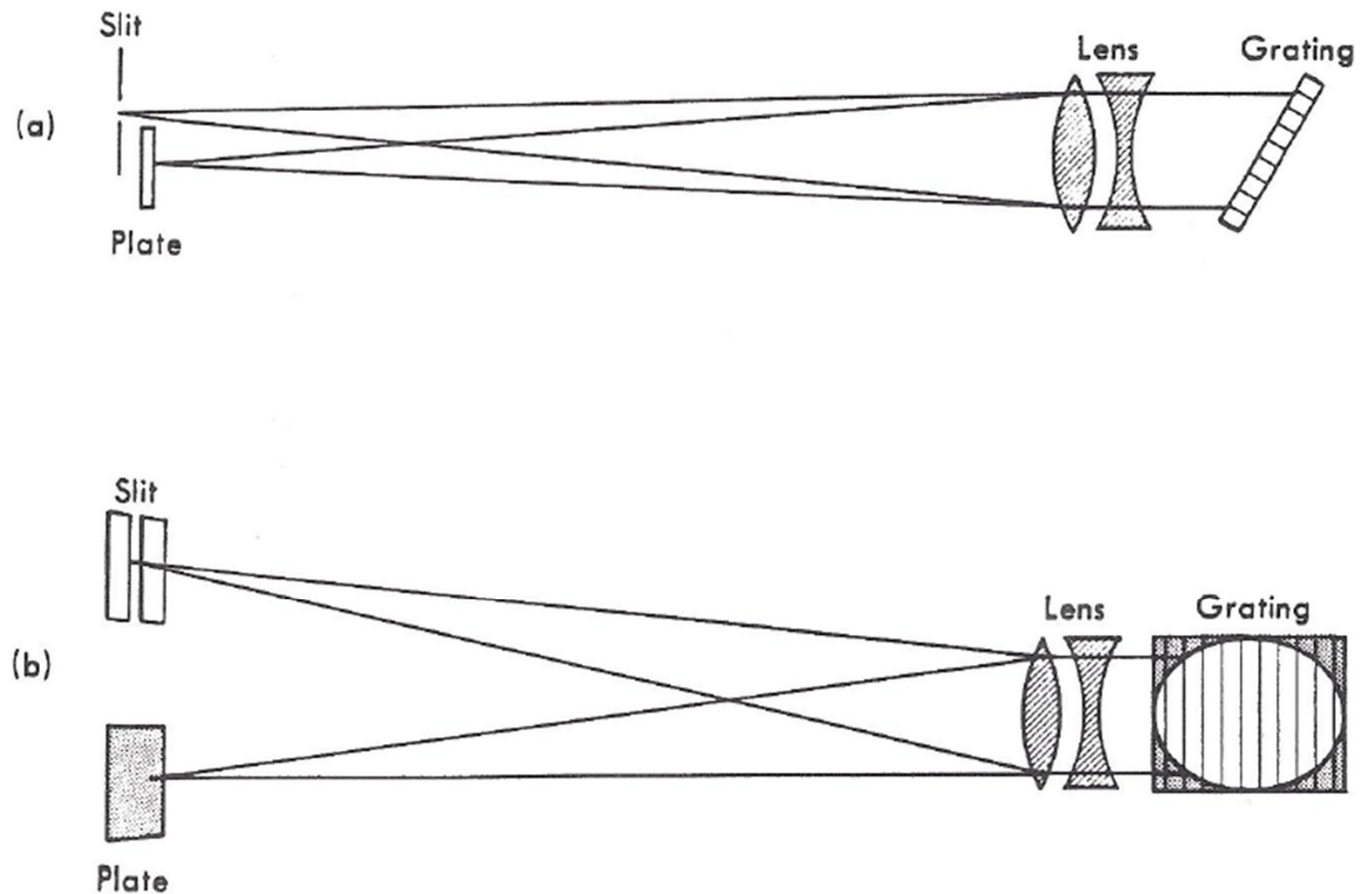


The first standard grating is optimized for a single lower order. The echelle is mounted orthogonally in such a way that the highly illuminated orders of the echelle are transversally separated. Different parts of the spectrum are recorded simultaneously.

# Littrow spectrograph

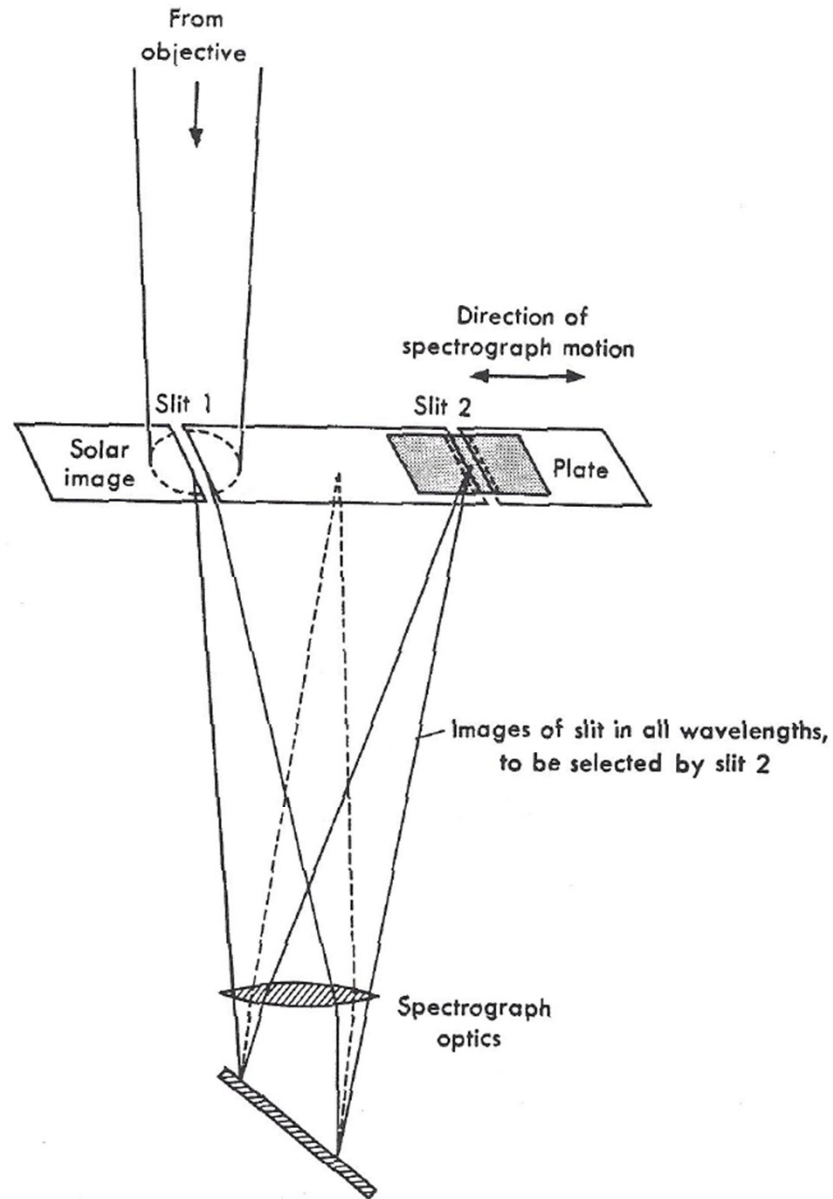
In the Littrow system, a single lens perform functions of both collimator and camera

2.7. The Littrow spectrograph, a simple arrangement utilizing a single lens for both collimator and camera. The slit and plate are both at the focus of the lens. Its symmetry makes it convenient for rotating spectrographs, but the use of a lens introduces chromatic aberration, which must be corrected by tilting the camera plane. The system is viewed (a): parallel to the slit and (b): perpendicular to the slit, which is always parallel to the grating lines. The  $f$ /ratio of the collimator must match that of the telescope.



# Spectroheliograph

2.8. Optical diagram of the spectroheliograph. The spectrograph produces monochromatic images of the slit in all wavelengths. If the slit is moved across the Sun, images of the Sun in all wavelengths are built up. Slit 2 picks out a single wavelength, producing a monochromatic image of the Sun on the plate, which is held fixed. Pictures may be made in any wavelength, with arbitrary pass band. Exposures are long, because only a small fraction of the Sun is photographed at any time; but the exposure for any single element on the surface is short.

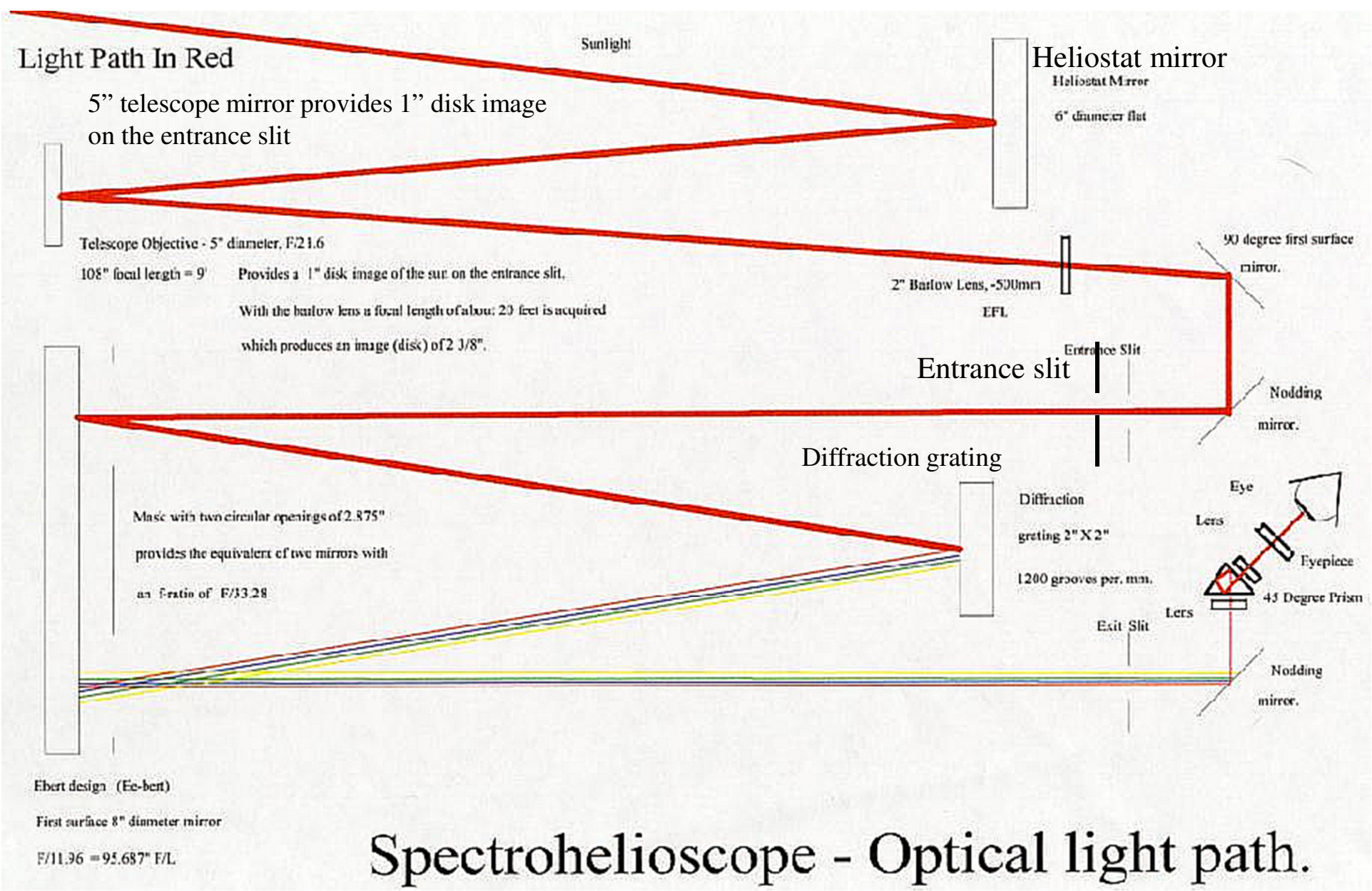


## **Spectrohelioscope.org**

The instrument is built by Leonard Higgins in Sonoma county. "The instrument is a pleasure to use, and provides many different aspects and challenges in regard to observing the closest star, our sun."



[Spectrohelioscope.org](http://Spectrohelioscope.org)



# Spectroheliometer - Optical light path.

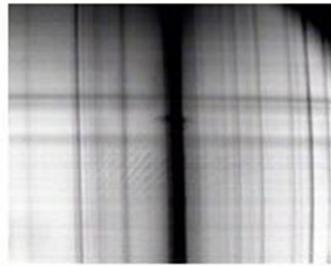
**The optical scheme. Telescope Objective 5",  $f = 108"$ , diffraction grating 2" x 2", 1200 grooves per mm.**

# Examples of Spectrohelioscope observations

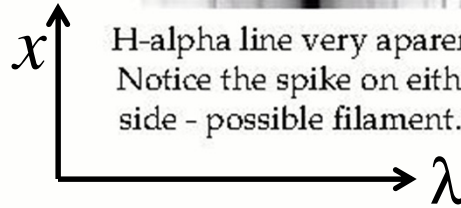


Horizontal lines are due to sunspots

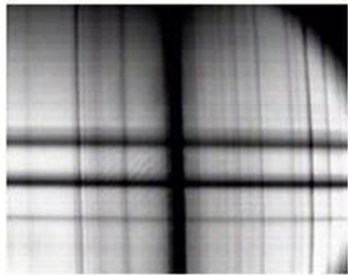
In the deep red beyond the B line.



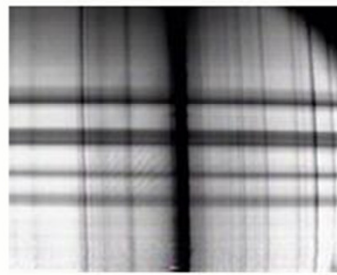
H-alpha line very apparent  
Notice the spike on either side - possible filament.



Solar spectra taken on June 27, 1999.



You can see the umbra and penumbra of the sunspot.



Many sunspots and much detail to observe.

K line of Ca



C line of Fe



C line of Fe



Views of the sun's disk with mirror synthesizer operating.

**Exercise.** Estimate the spectral resolution of Leonard Higgins's spectrohelioscope.

# The Interface Region Imaging Spectrograph (IRIS)

IRIS observes UV spectra of the chromosphere-corona transition region: 19 cm telescope, spatial resolution 0.33 arcsec, field of view 175x175 arcsec<sup>2</sup>

B. De Pontieu *et al.*

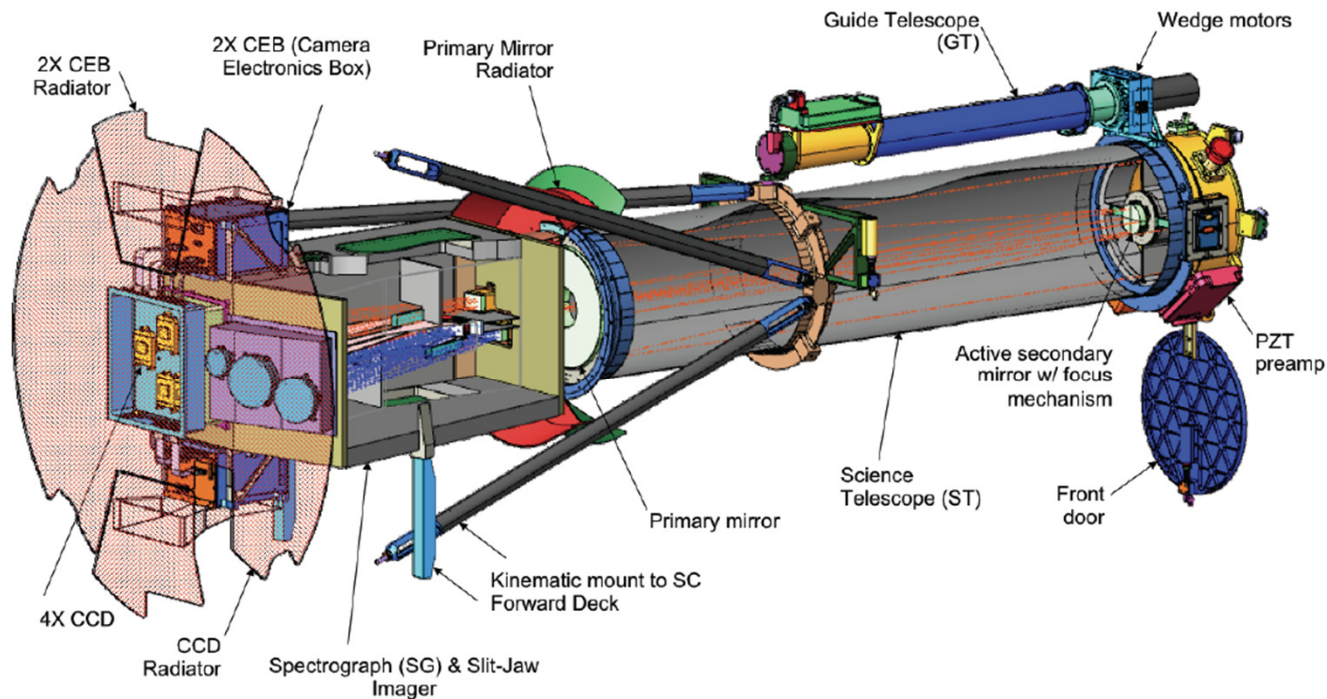


**Figure 8.** Conceptual design of the IRIS instrument. Sunlight enters from the right. For the flight design the telescope and guide telescope assemblies are rotated 180 degrees about the instrument axis relative to the spectrograph box (see Figure 7).

# IRIS spectrograph

The instrument simultaneously obtains spectra and slit-jaw images (images reflected from the spectrograph slit) in the Near-UV and Far-UV spectral intervals.

The Czerny-Turner design separates collimator and camera mirrors.

*Interface Region Imaging Spectrograph*

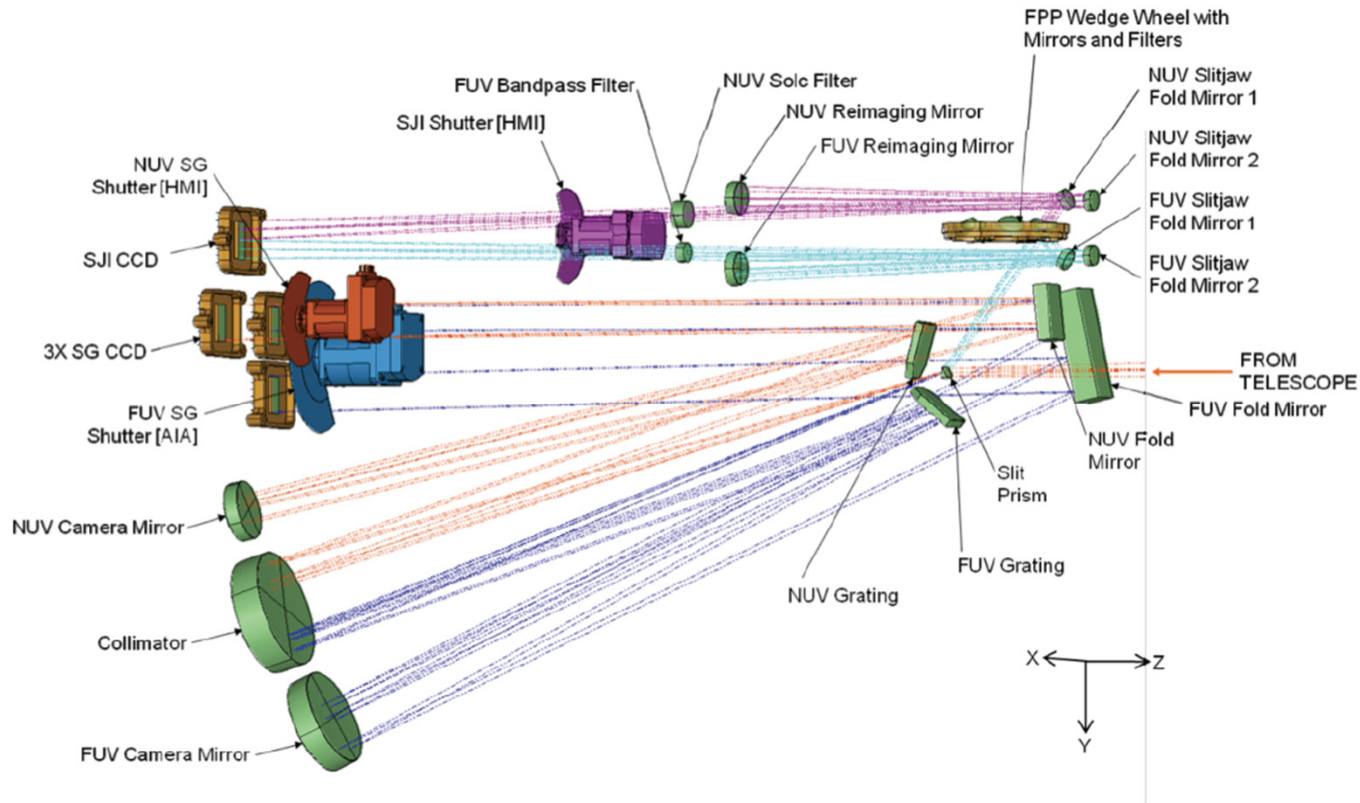
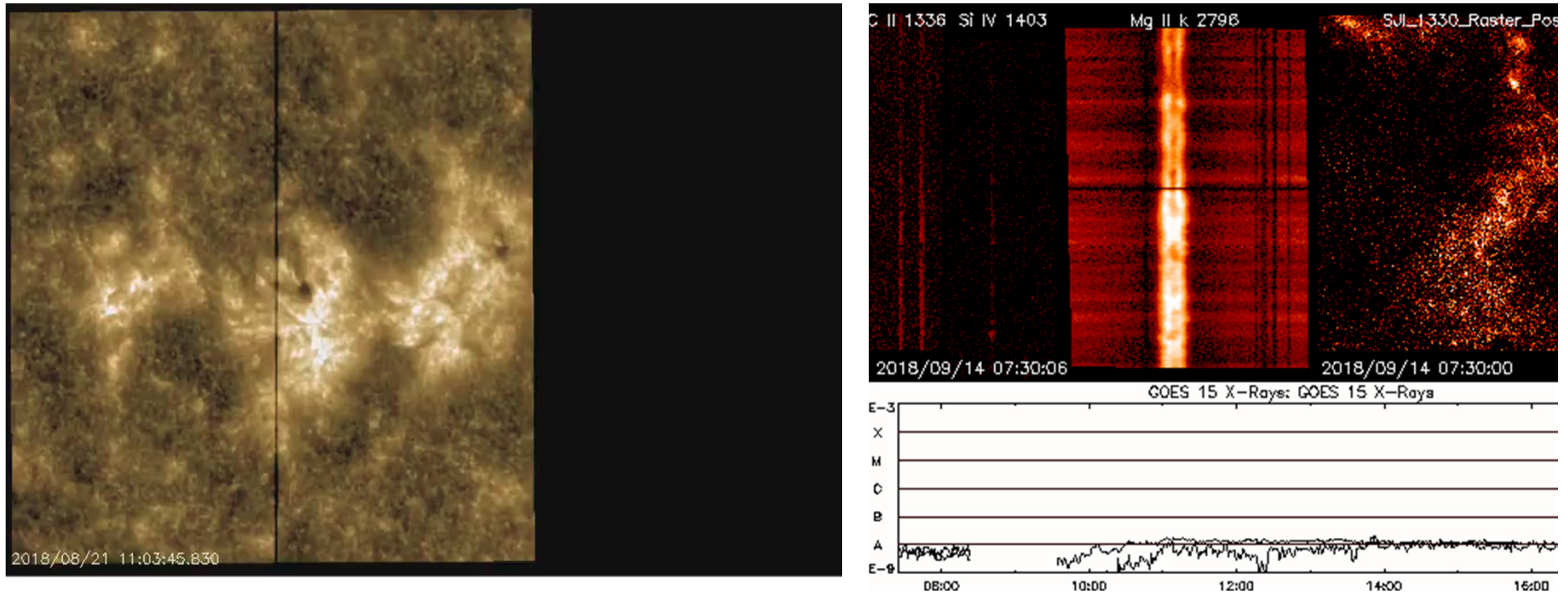


**Figure 9.** Path taken by light in the FUV spectrograph (dark blue), NUV spectrograph (orange), FUV slitjaw (light blue) and NUV slitjaw (purple) path.

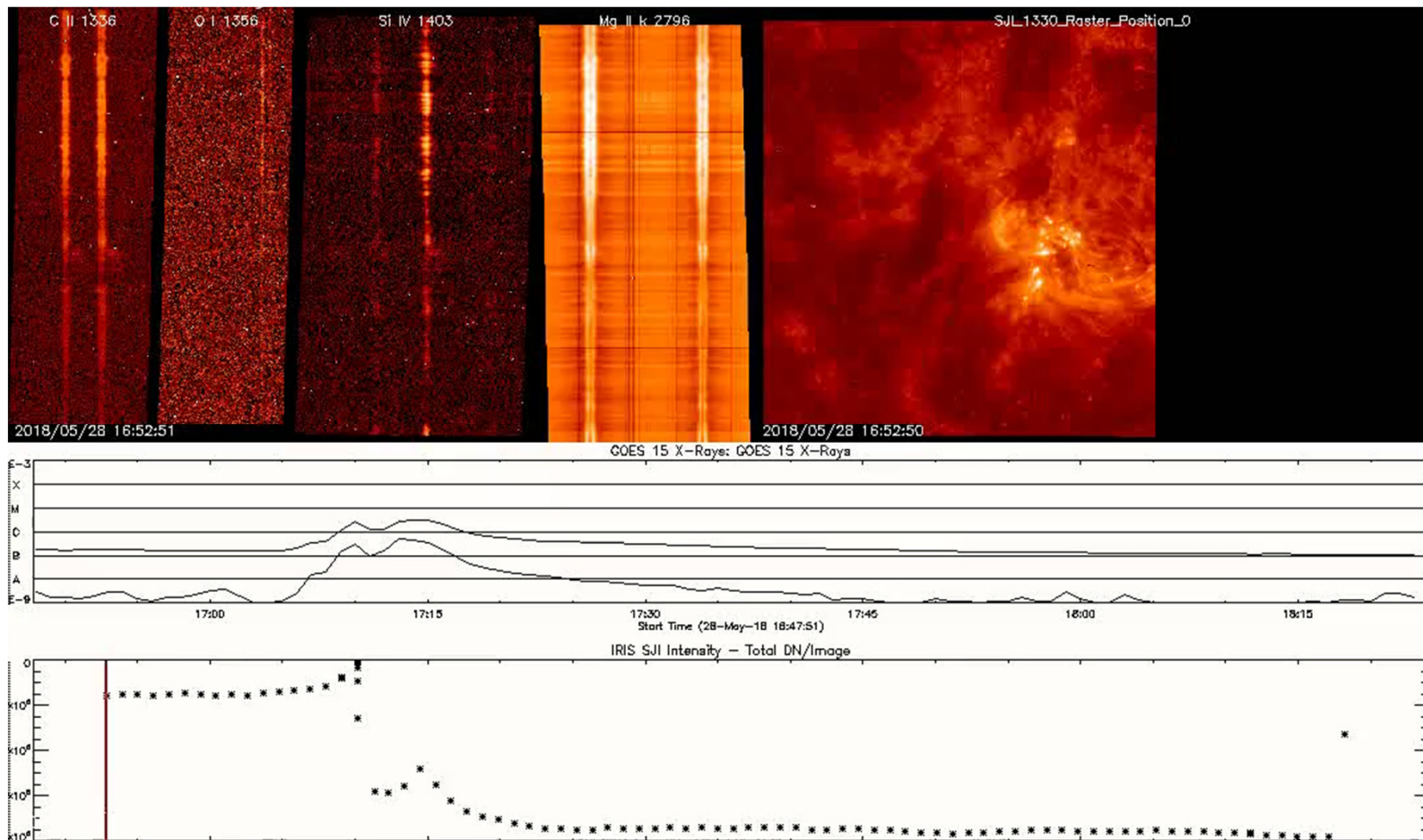
# IRIS observations on 08/21/18-09/14/18



This Mg II k (279.6 nm) slit-jaw movie shows NOAA AR 12719 making its way across the disk, starting three days after the region had emerged. While active at first, the active region seems to be decaying in the first half of the movie, but then magnetic fields suddenly start emerging bringing new life to the scene. The heating that is released while the magnetic fields reconfigure leads to short-lived brightenings, both compact and in more elongated filamentary structures, as the two opposite polarity pores (dark, roundish spots) move apart. Eventually the build up of magnetic potential energy is sufficient to be released in a minor flare visible towards the end of the movie.

# C2.7 flare of 05/28/18 observed by IRIS

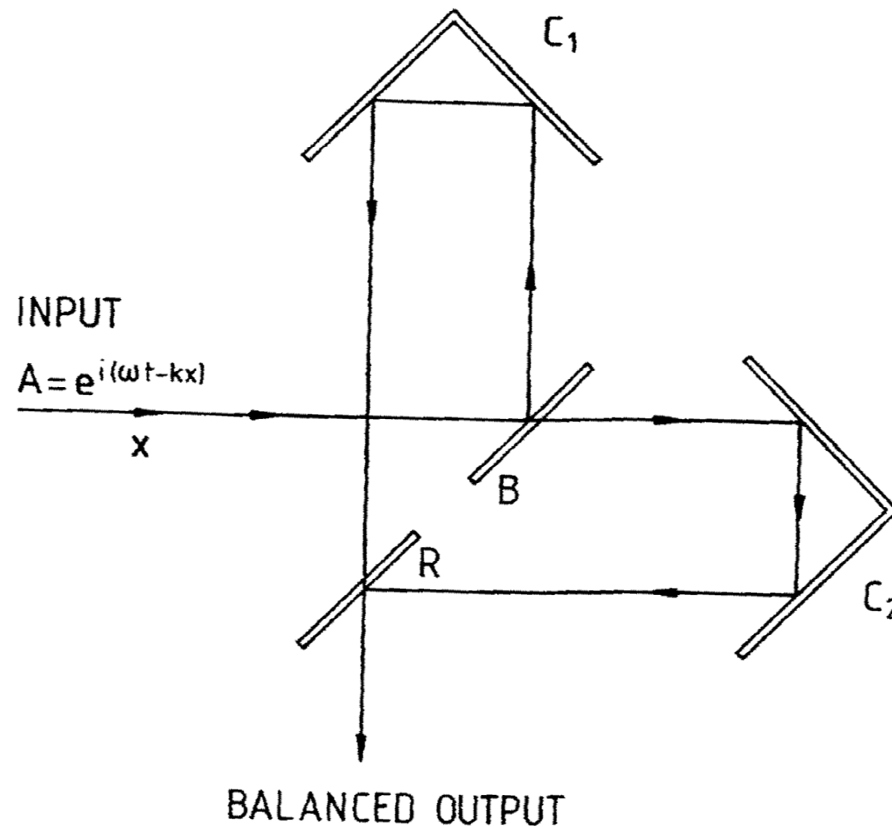
The C2.7 flare is prominently visible in the C II slit-jaw movie in the top right, shooting out material that later falls back to the surface again along arched trajectories, both towards the leading part of the active region on the right and the trailing part on the left, where the flare occurred. The IRIS slit crosses the flare exactly as it goes off, catching the strong broadening and enhancement of all the major lines (C II, Si IV and Mg II h & k), as well as the usually weaker lines (like O I and C I) that IRIS routinely observes.



# Fourier Transform Spectrometer.

In solar spectral observations interferometers are often used instead of gratings.

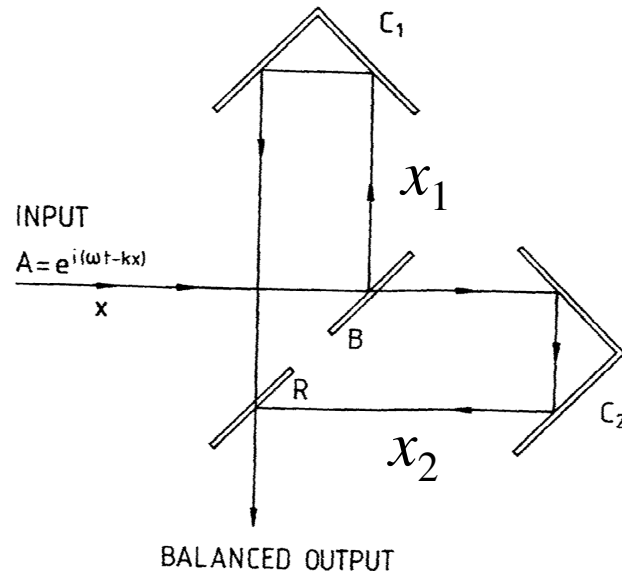
Fourier Transform Spectrometer is essentially a Michelson interferometer.



**Fourier Transform Spectrometer.  $C_1$  and  $C_2$  are retroreflectors,  $B$  beamsplitter,  $R$  recombiner.**

# Fourier Transform Spectrometer

Consider the 'balanced' output the interferometer:



$$A = r_c r_e \tau e^{i\omega t} \left( e^{-ikx_1} + e^{-ikx_2} \right),$$

where  $r_c$  is the reflection coefficient of  $C_1$  and  $C_2$ ,  $r_e$  and  $\tau$  are the reflection and transmission coefficients of the recombiner  $R$ ,  $k = 2\pi/\lambda$ ,  $x_1$  and  $x_2$  are the lengths of the two paths.

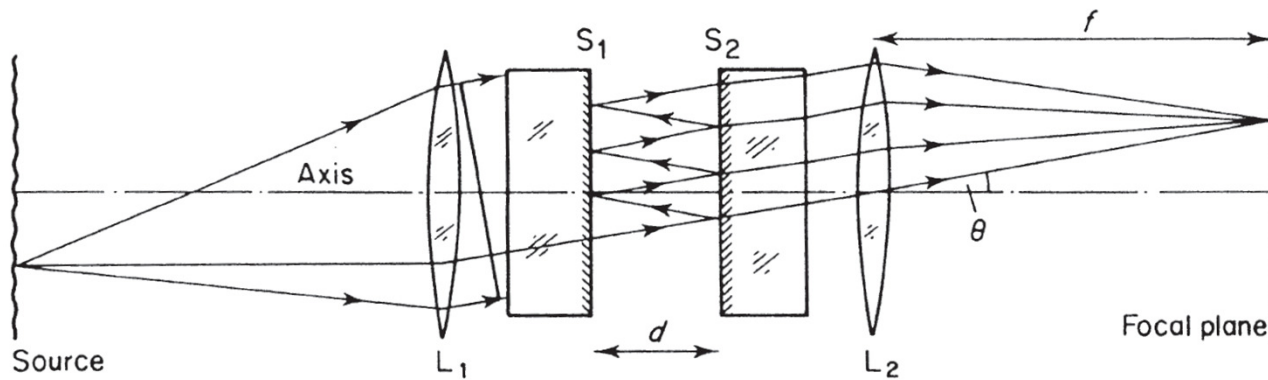
The emergent intensity is:  $I = A^* A = \frac{\eta}{2} [1 + \cos k(x_2 - x_1)]$ ,

where  $\eta = 4r_c^2 r_e^2 \tau^2$  is the efficiency of the instrument. In general, the input is not monochromatic. If it has an intensity spectral distribution  $B(k)$  then the output signal is:

$$I(x) = I_0 + \frac{1}{2} \int_0^\infty \eta B(k) \cos(kx) dk, \quad \text{where } x = x_2 - x_1.$$

The spectral intensity can be recovered by the inverse Fourier transform if  $I(x)$  for a range of  $x$  is measured.

## Fabry-Perot interferometer (etalon)



An incident beam is multiply reflected between the two parallel surfaces, but with each reflection a fraction  $R$  of the intensity is reflected and a fraction  $T$  is transmitted, and all these transmitted fractions interfere in the outgoing beam.

If the angle of incidence is  $\theta$ , the layer thickness is  $d$ , the refraction index is  $n$ , then the path difference between two successive beam fractions is  $\Delta = 2nd \cos\theta$ , and the phase difference is  $\delta = 2\pi\Delta/\lambda = 4\pi nd (\cos\theta)/\lambda$ .

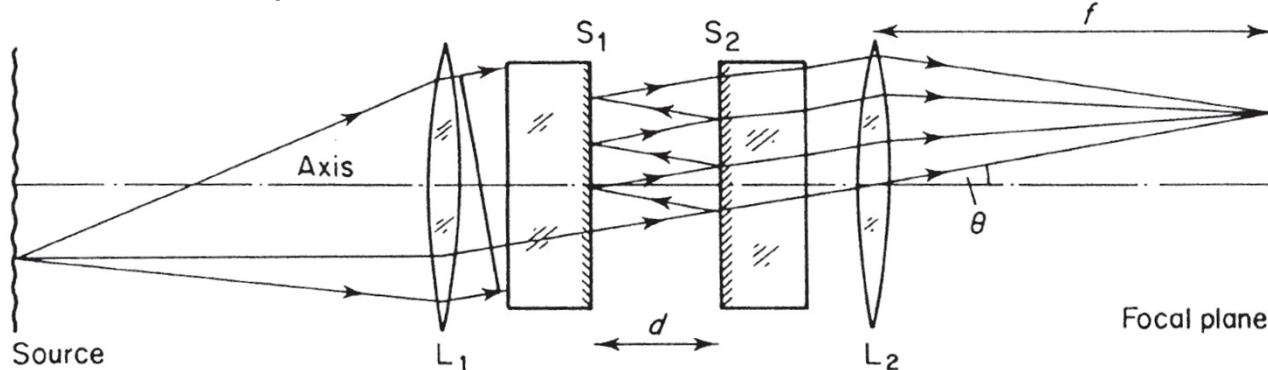
For an incoming wave of form  $\exp(i\omega t)$  the transmitted and reflected (absolute) wave amplitudes are  $T^{1/2}$  and  $R^{1/2}$ , respectively; thus, counting all the reflections and the phase differences, the outgoing wave is a geometric series:

$$Ae^{i\omega t} = Te^{i\omega t} + TRe^{i(\omega t + \delta)} + TR^2e^{i(\omega t + 2\delta)} + \dots$$

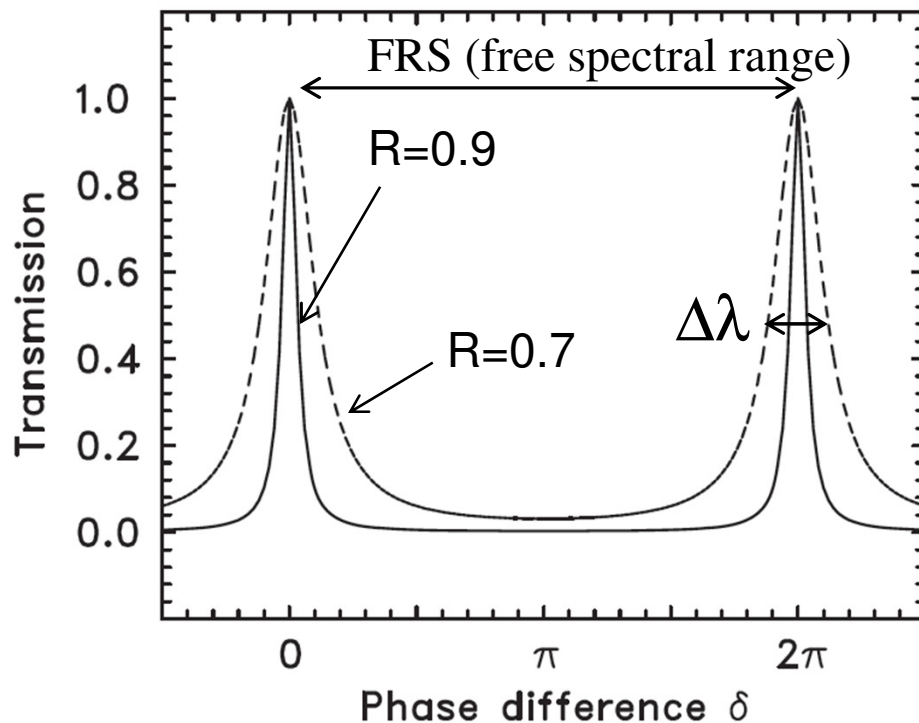
$$A = T(1 + Re^{i\delta} + R^2e^{2i\delta} + \dots) = T/(1 - Re^{i\delta})$$

$$I = AA^* = \frac{T^2}{1 - 2R \cos \delta + R^2} = \frac{T^2}{(1 - R)^2 + 4R \sin^2(\delta/2)}$$

# Fabry-Perot interferometer (etalon)



$$I = AA^* = \frac{T^2}{1 - 2R \cos \delta + R^2} = \frac{T^2}{(1 - R)^2 + 4R \sin^2(\delta/2)}$$



The transmission is periodic; the  $m$ th maximum is at  $\delta = 2m\pi$  or  $\lambda = 2nd \cos\theta/m$ . The distance between the peaks (**Free Spectral Range**) is  $\text{FRS} = \lambda/m = \lambda^2/2nd \cos\theta$ . Full-width at half maximum (**FWHM**),  $\Delta\lambda$ , depends on the reflectance  $R$ :

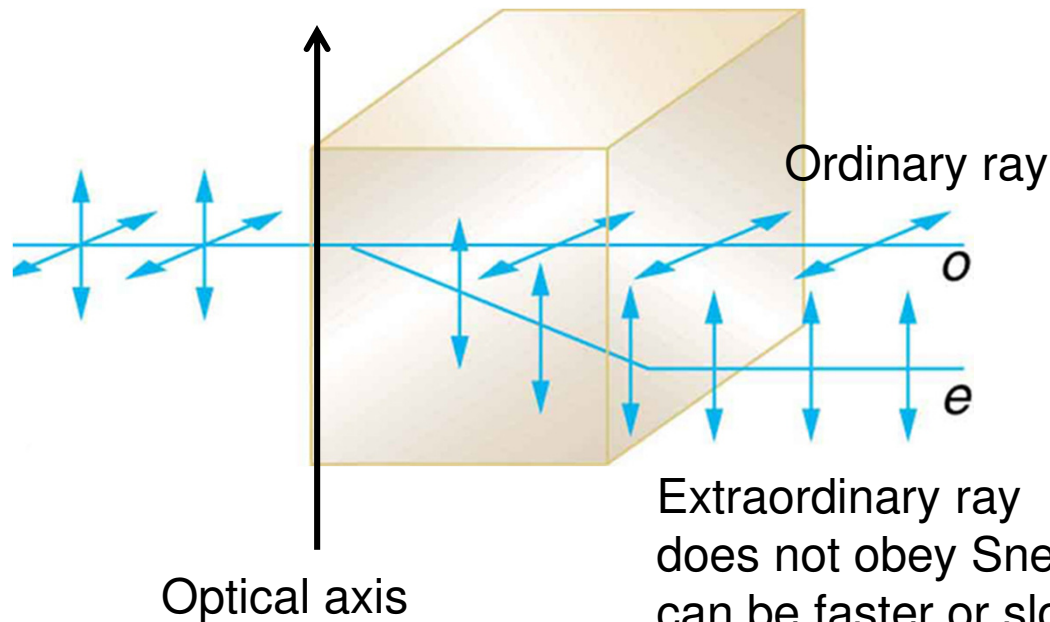
$$\Delta\lambda = \frac{(1 - R)\lambda^2}{2\pi nd \cos\theta \sqrt{R}}$$

The ratio,  $\text{FRS}/\Delta\lambda$  is called *finesse*. For  $\lambda=500\text{nm}$ ,  $d=1\text{mm}$ ,  $\text{FRS}=0.13\text{nm}$  small. Thus, Fabry-Perot etalons are used in combination with other filters.

## Polarization Filters

### Birefringent Filters.

An optically anisotropic, birefringent medium (quartz, calcite) can be used to produce a relative delay between ordinary and extraordinary rays aligned along the fast and slow axes of the crystal. A birefringent medium has two different refractive indices, depending on the plane of light propagation through the medium. The two rays are polarized in mutually perpendicular planes.



Extraordinary ray  
does not obey Snell's law,  
can be faster or slower than the o-ray.

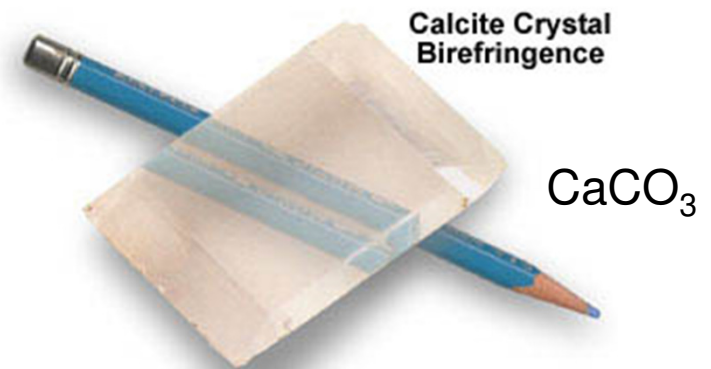
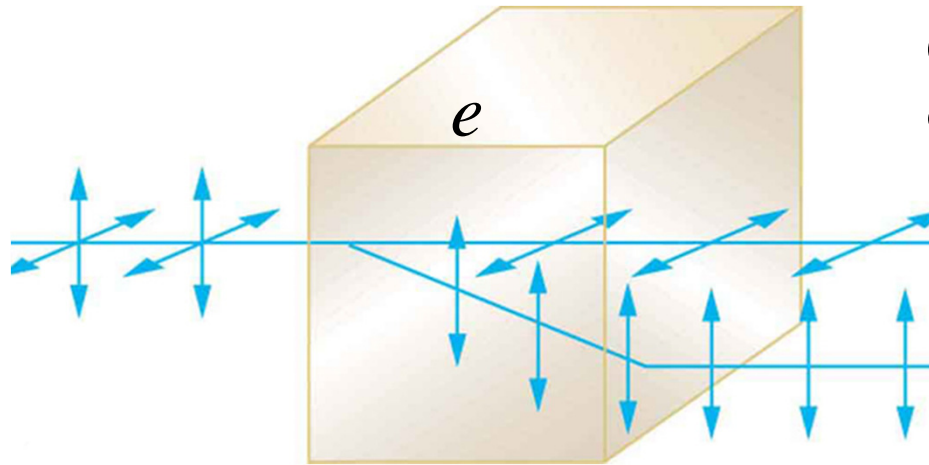


Figure 2



Calculate the phase difference between ordinary and extraordinary rays:

$$\phi_o = \frac{\omega}{c} n_o e = \frac{2\pi}{\lambda} n_o e \quad n_o = 1.6584$$

$$\phi_e = \frac{\omega}{c} n_e e = \frac{2\pi}{\lambda} n_e e \quad n_e = 1.4864$$

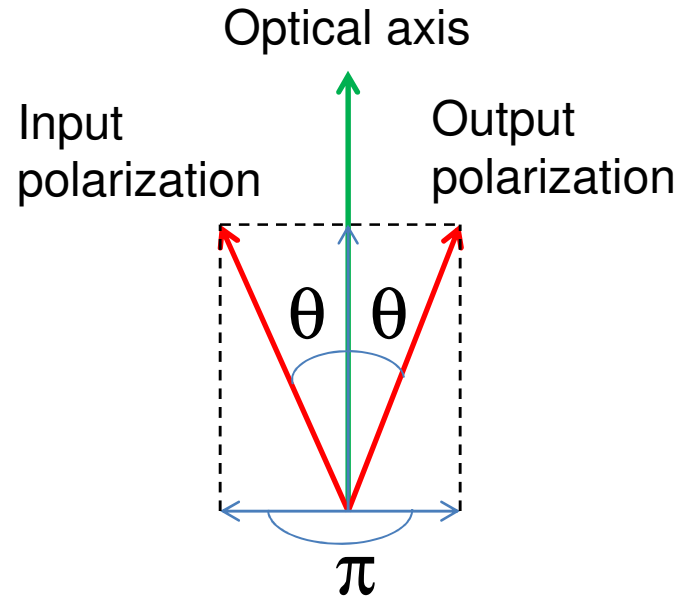
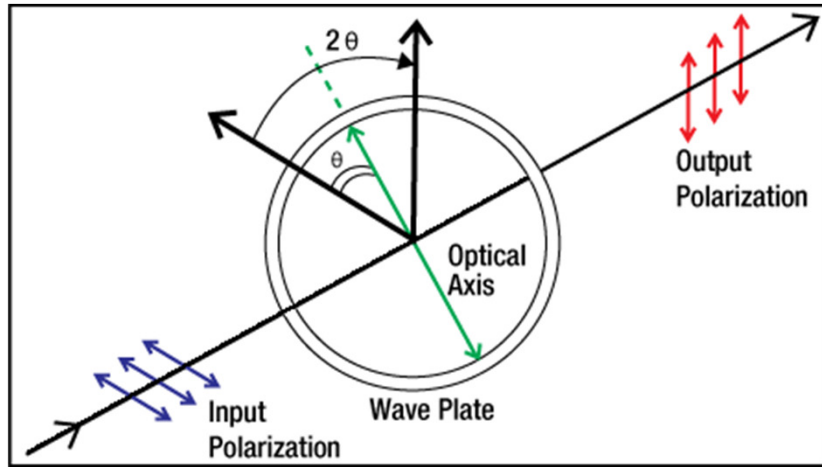
The phase difference between the ordinary and extraordinary rays propagating through a birefringent crystal of thickness  $e$  is:

$$\delta = \frac{2\pi}{\lambda} e(n_o - n_e) = \frac{2\pi e J}{\lambda},$$

where  $n_o$  and  $n_e$  are the refraction coefficients of the ordinary and extraordinary rays,  $\lambda$  is the wavelength. The difference  $n_o - n_e \equiv J$  is sometimes called the '*birefringence*'.

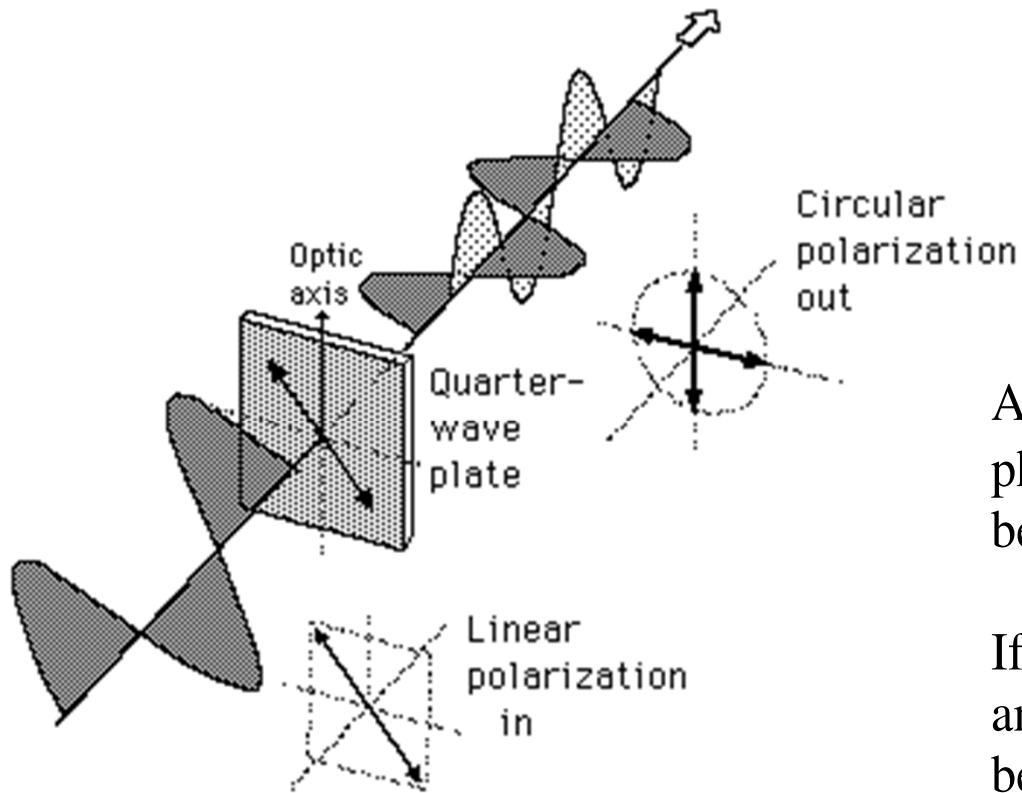
When  $\delta = \pi/2$  the filter is called  $\lambda/4$  retarding plate (*quarter-wave plate*); for  $\delta = \pi$  the filter is called  $\lambda/2$  plate (*half-wave plate*).

# Half-wave plate



A half-wave plate introduces a phase difference of  $\pi$  radians between perpendicular axes. Rotating a half wave plate by an angle  $\theta$  relative to the polarization direction of linearly polarized light will therefore shift its polarization angle by  $2\theta$ . This can be observed by placing a half-wave plate at angle  $45^\circ$  between crossed polaroids, and noting that light is transmitted.

## Quarter-wave plate



A quarter-wave plate introduces a phase difference of  $\pi/2$  radians between perpendicular axes.

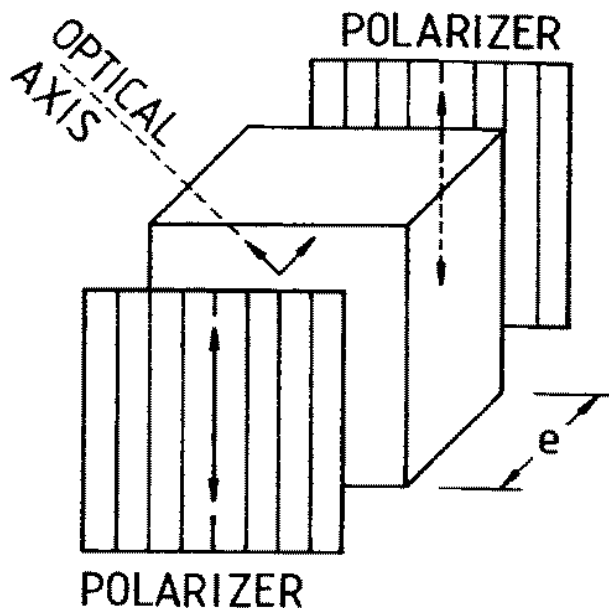
If a quarter-wave plate is placed at  $45^\circ$  angle to linearly polarized light, it will be converted to circular.

If linearly polarized light is incident on a quarter-wave plate at  $45^\circ$  to the optical axis, then the light is divided into two equal electric field components.

One of these is retarded by a quarter wavelength by the plate. This produces circularly polarized light. Incident circularly polarized light will be changed to linearly polarized light.

# Polarization filter.

Consider a birefringent crystal with two linear polarizers on both sides with the polarization axis at 45 degrees to the optical axis of the crystal.



The linear polarized wave of amplitude  $A$  becomes decomposed in the crystal into two perpendicular waves of amplitude  $A/\sqrt{2}$ .

The second polarizer transmits only components parallel to its axis. The amplitude of these components is  $A/2$ .

Therefore, the combined signal is:

$$\frac{A}{2} \cos(\phi + \delta) + \frac{A}{2} \cos \phi = A \cos \frac{\delta}{2} \cos \left( \phi + \frac{\delta}{2} \right),$$

where  $\phi$  is a common phase of the components.

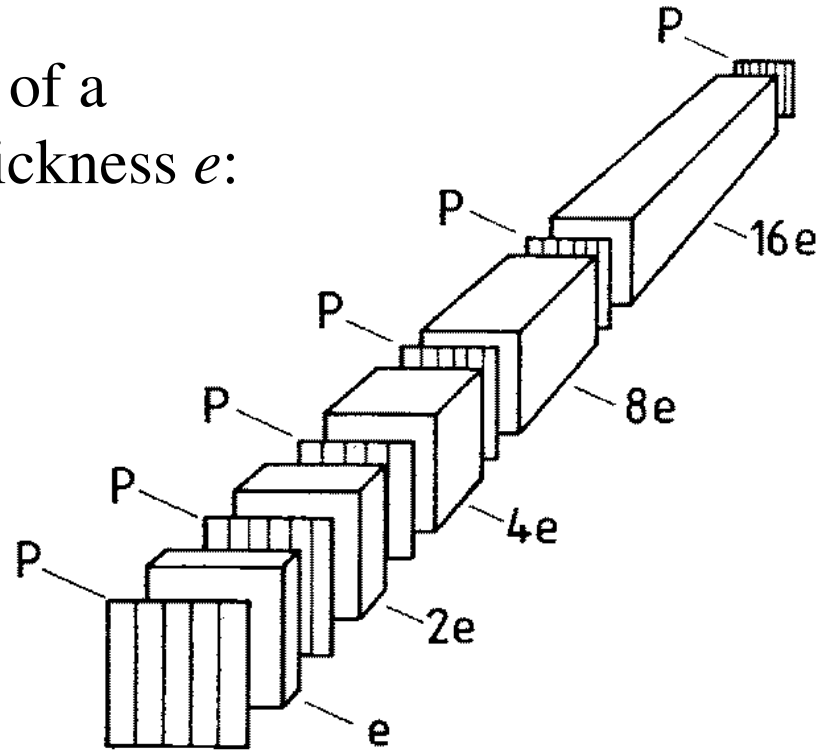
The output intensity is modulated with wavelength  $\lambda$ :  $I = A^2 \cos^2 \frac{\delta}{2} = A^2 \cos^2 \frac{\pi e J}{\lambda}$ .

Intensity has maxima at  $\delta = 2k\pi$ , or  $\lambda = eJ / k$ .

## Lyot filter.

Passing intensity of a single filter of thickness  $e$ :

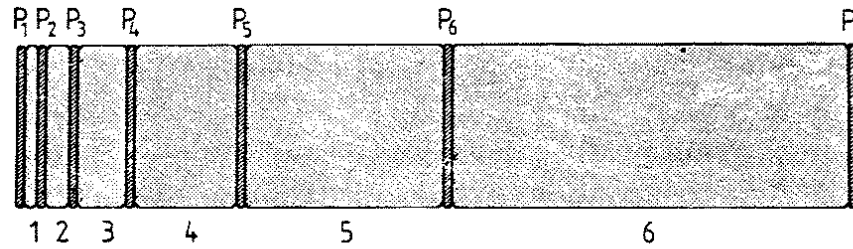
$$I = A^2 \cos^2 \frac{\pi e J}{\lambda}.$$



**Lyot filter consists of  $N$  filter components of increasing thickness  $e$ ,  $2e$ ,  $4e$ , ...**

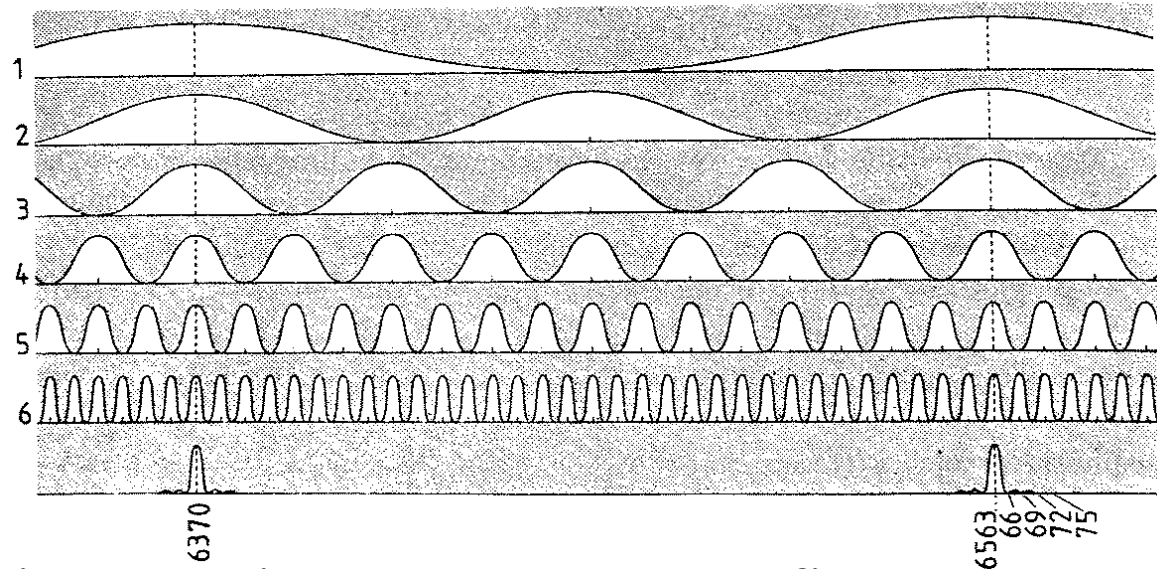
The passing intensity of the Lyot filter is:

$$I = A^2 \cos^2 (\pi e J / \lambda) \cos^2 (2\pi e J / \lambda) \dots \cos^2 (2^{N-1} \pi e J / \lambda).$$



$$I_1 = A^2 \cos^2 \frac{\pi e J}{\lambda}$$

$$I_N = A^2 \cos^2 \frac{2^{N-1} \pi e J}{\lambda}$$



### Intensity transmitted through the Lyot filter.

The locations of the maxima are determined by the thinnest filter, and the bandwidth is determined by the thickest filter:

$$\lambda = eJ / k_1, \text{ for the thinnest filter}$$

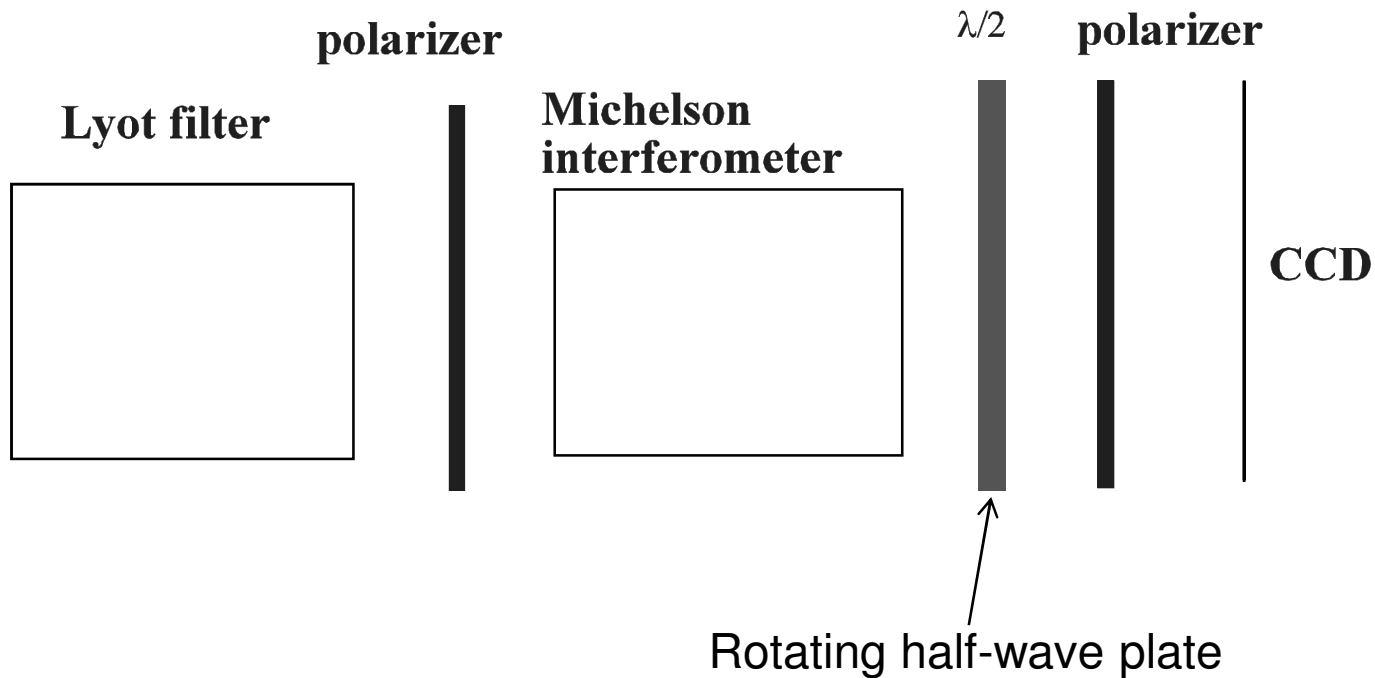
$$\lambda = 2^{N-1} eJ / k_N, \text{ for N-filter}$$

$$\Delta\lambda / \lambda \approx 1 / k_N, \text{ - bandwidth of filter N}$$

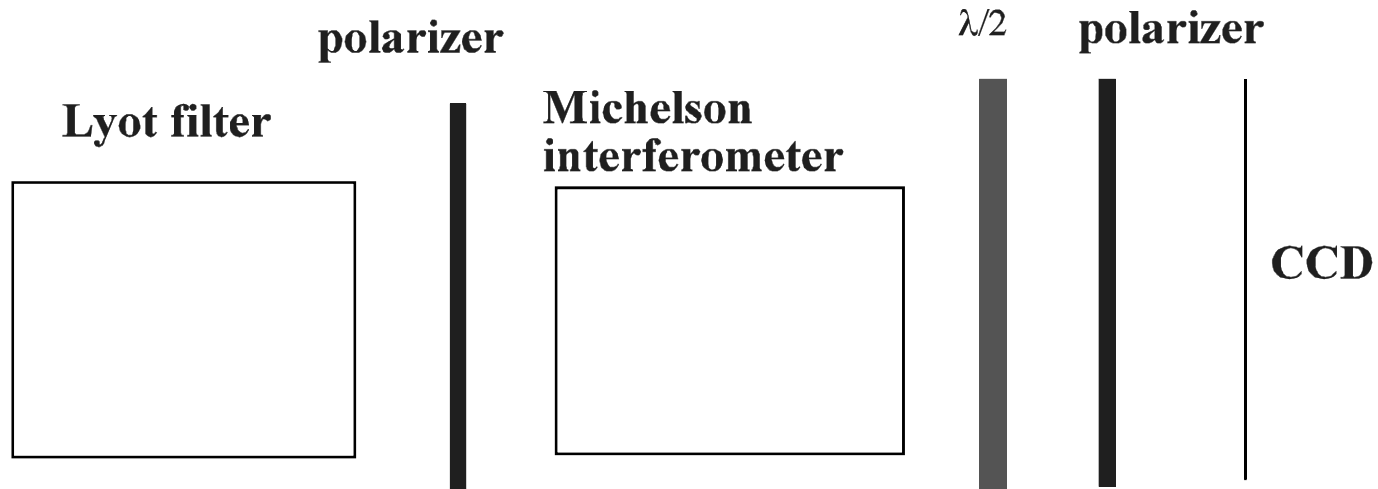
$$\text{Then } \Delta\lambda / \lambda \approx \frac{\lambda}{2^{N-1} eJ}$$

## Fourier Tachometer

Fourier tachometer measures the Doppler line shift. It consists of Lyot filter, Michelson interferometer, rotating half-wave plate, polarizers and CCD detector.



**A scheme of Fourier Tachometer.**



The signal coming through the Michelson interferometer is modulated:

$$I \propto 1 + \cos[k(x_2 - x_1)] \equiv 1 + \cos(\phi),$$

where  $k = 2\pi/\lambda$  depends on the Doppler shift ( $\Delta k/k = -\Delta\lambda/\lambda$ ). To determine the Doppler shift one has to measure the phase shift  $\phi$ .

The rotating half-wave plate causes additional modulation:

$$I \propto \cos(2\theta + \phi) = \cos(4\omega t + \phi).$$

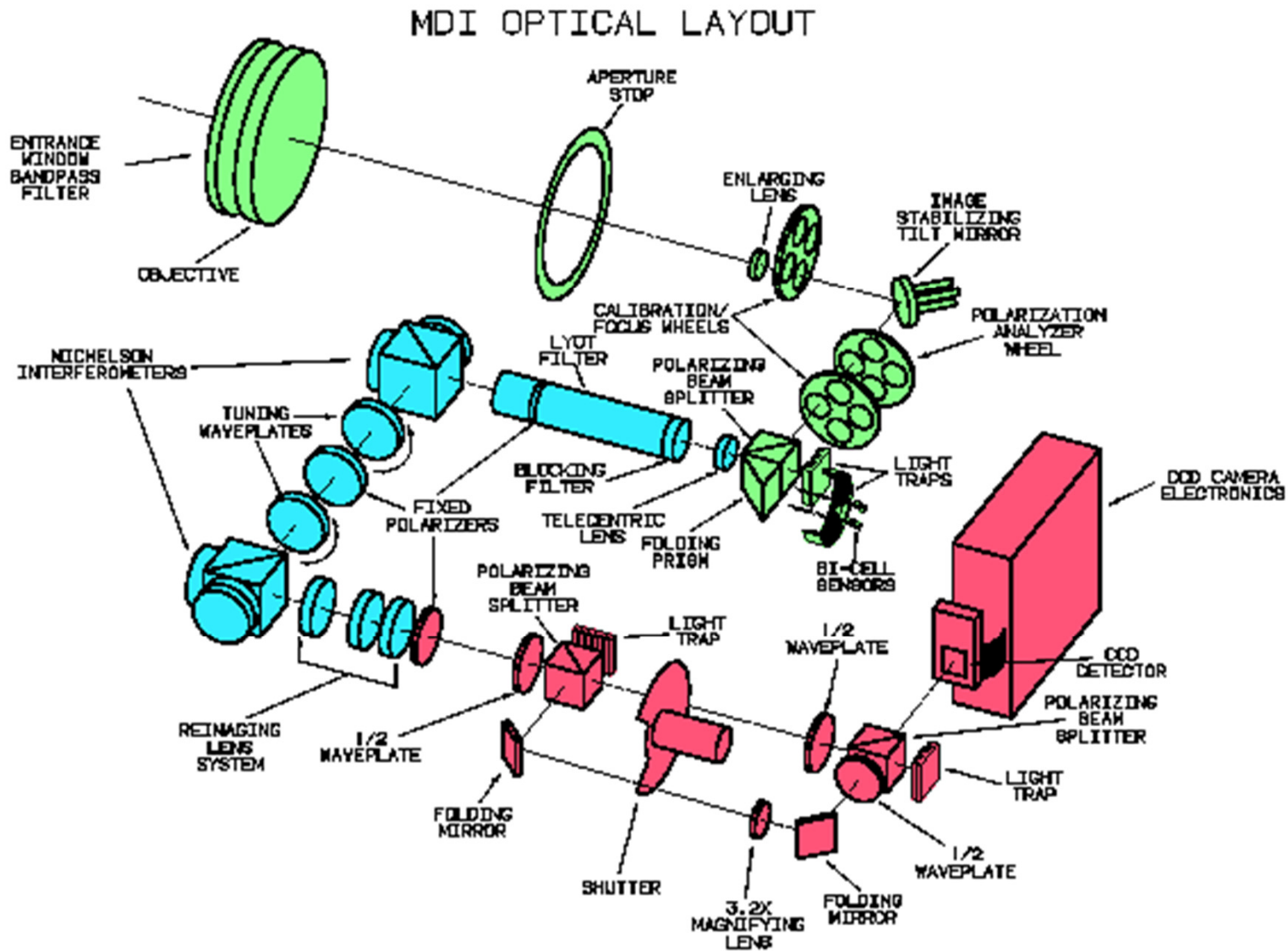
It is sufficient to measure the signal at three positions of the half-wave plate in order to determine  $\phi$ . For  $120^\circ$  intervals:

$$I_1 \propto \cos \phi, \quad I_2 \propto \cos(2\pi/3 + \phi), \quad I_3 \propto \cos(4\pi/3 + \phi).$$

Then,

$$\tan \phi = \frac{I_2 - I_3}{I_2 + I_3 - 2I_1}.$$

This principle is used in the helioseismology instruments, GONG (Global Oscillation Network Group) and MDI (Michelson Doppler Imager).



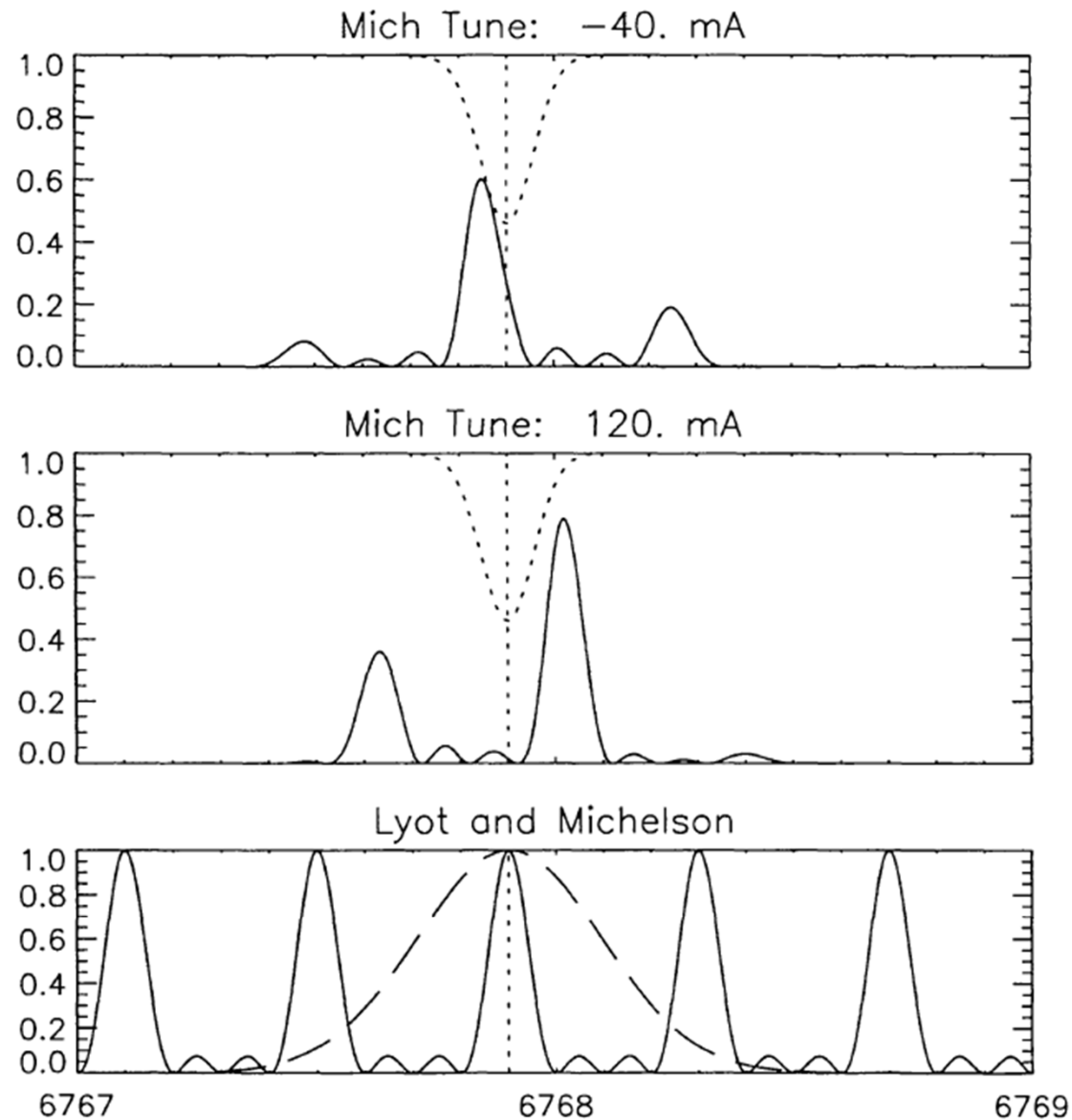
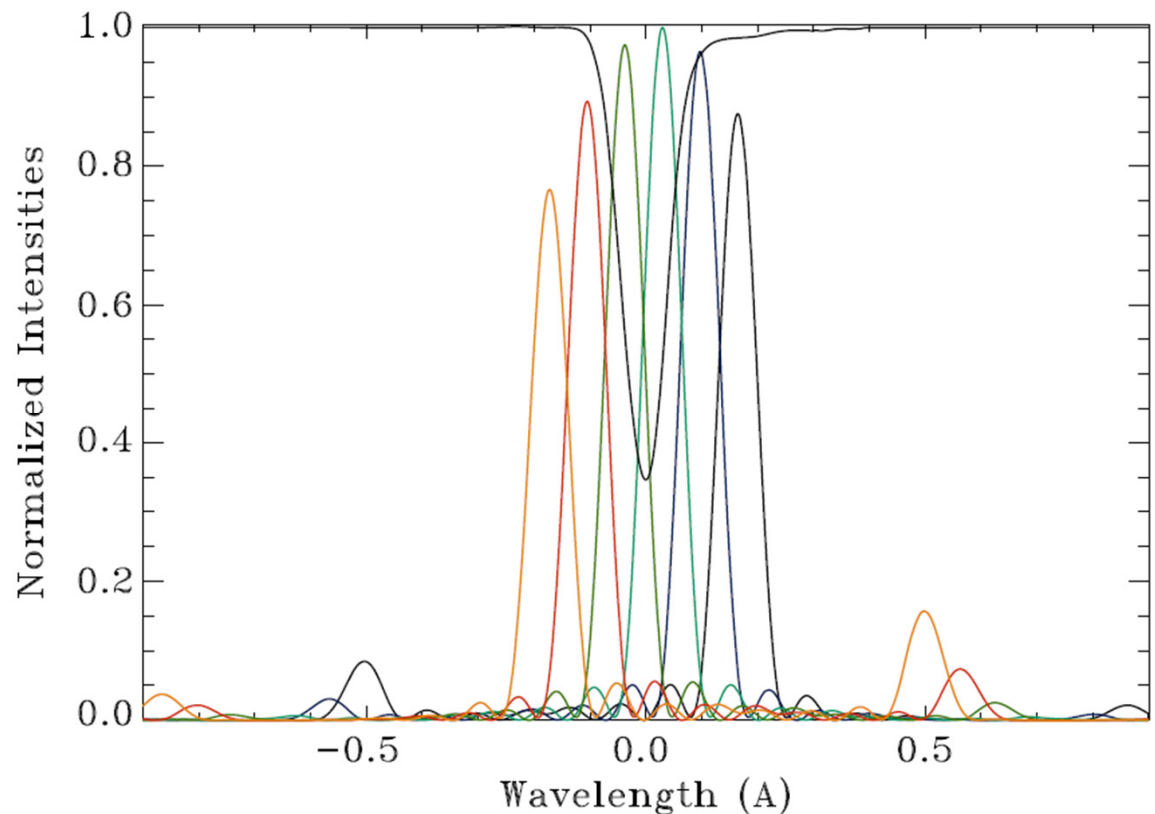


Fig. 7. MDI's principle of operation. The lower panel shows the individual profiles of the Lyot filter (dashed line) and the channel spectrum of both Michelsons in series (solid line). The upper panels illustrate the situation for two of the four nominal Doppler tunings. The solid line represents the resulting instrument transmission profile for the corresponding tuning position with respect to the 6768 Å line profile (dotted line).

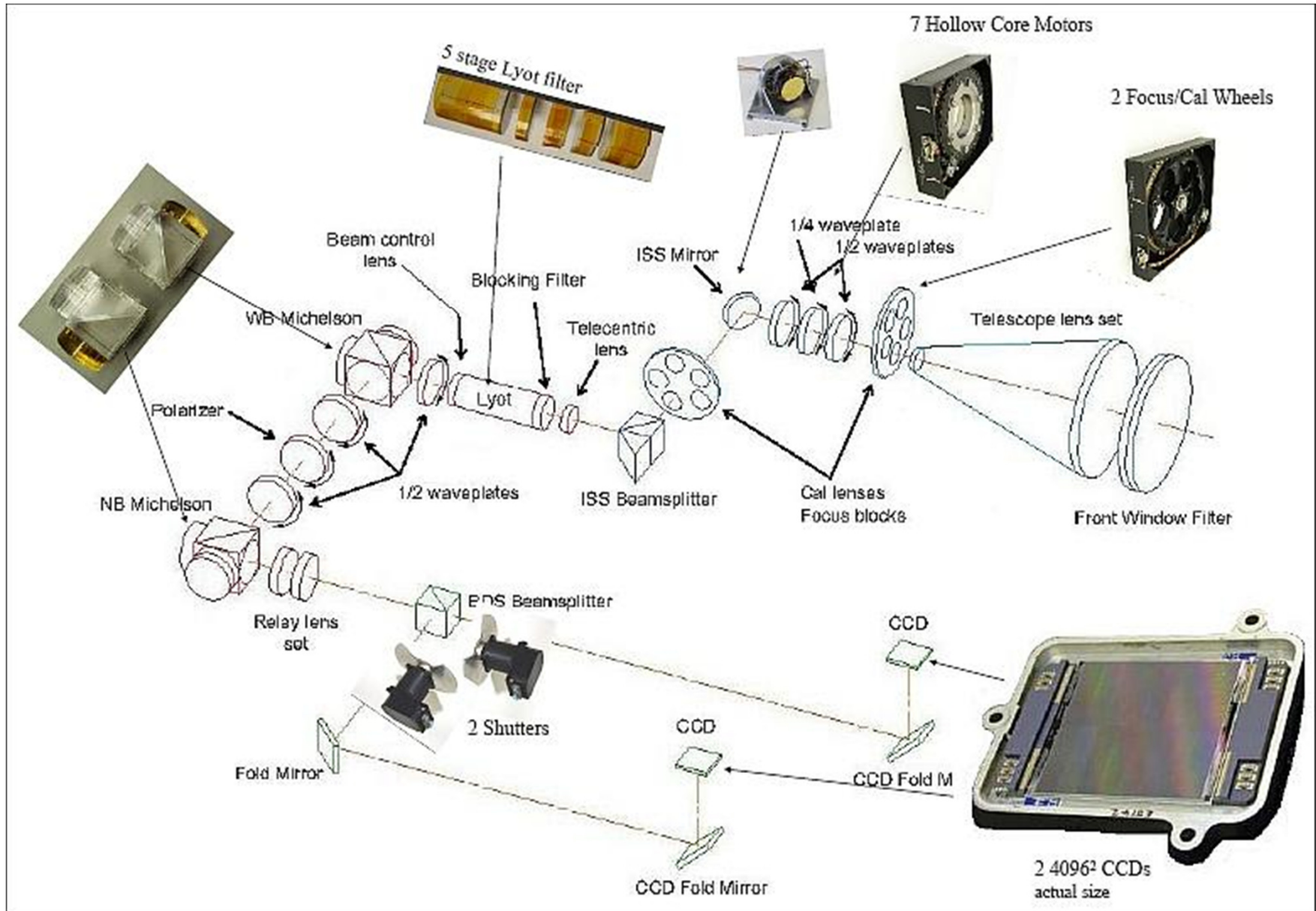
The Michelson Doppler Imager (MDI) on SOHO and Helioseismic and Magnetic Imager (HMI) on SDO are examples of the Fourier Transform Spectrometer. MDI measures  $I(\lambda)$  at 5 positions across the line (Ni I 6768Å), and HMI measures at 6 positions for Fe I (6173Å). The advantage of these type of measurements is that there is no need for a narrow entrance slit of the spectrometer.

Six tuning positions of the HMI instrument on Solar Dynamics Observatory (SDO) are shown here with respect to the Fe I 6173Å solar line at disk center and at rest.

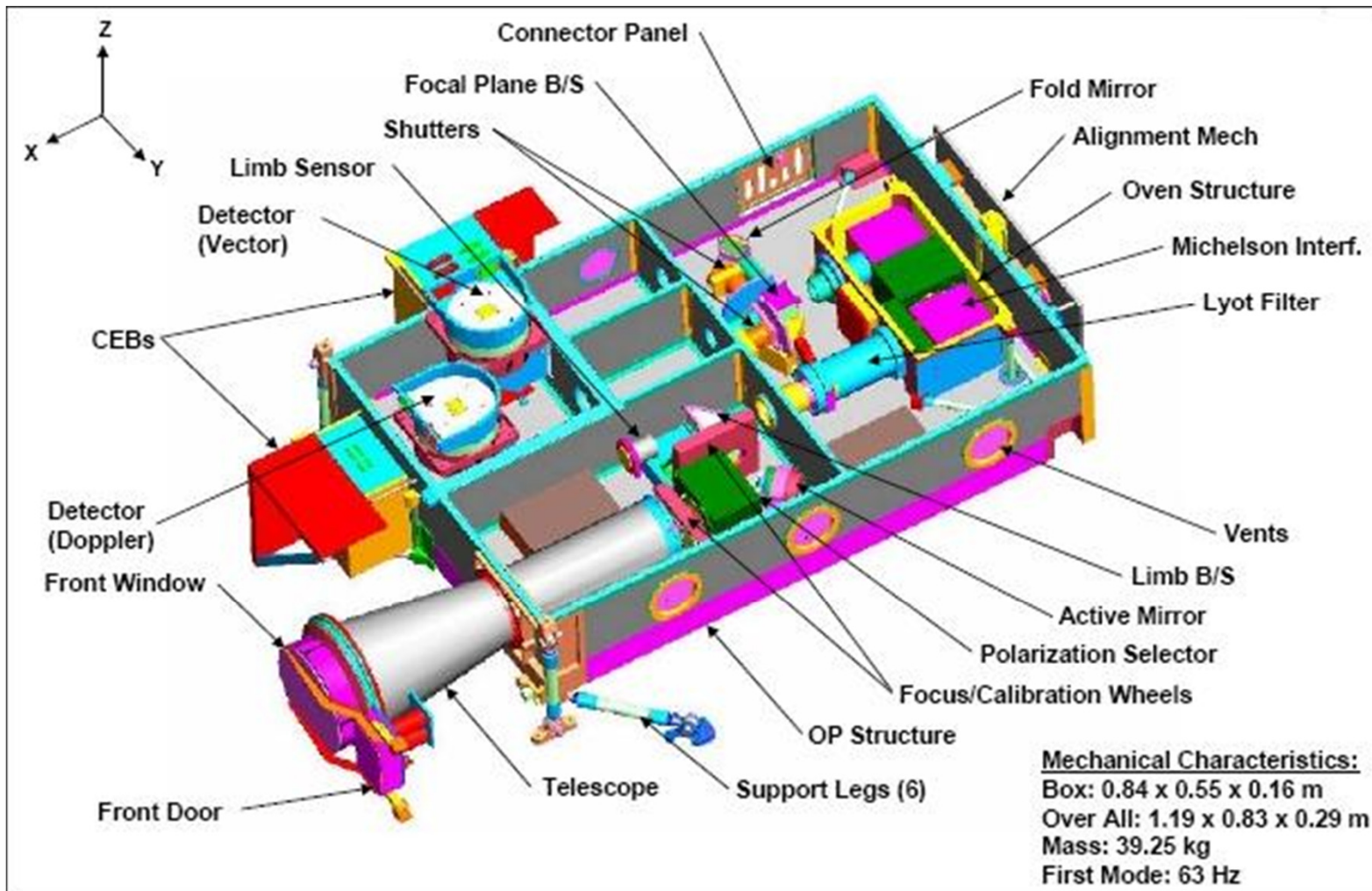
During observations the line profile is shifted due to the surface motions and spacecraft orbital velocity (Doppler effect), and also the line split in magnetic field (Zeeman effect). These line changes are used to measure the Doppler velocity and magnetic field strength.



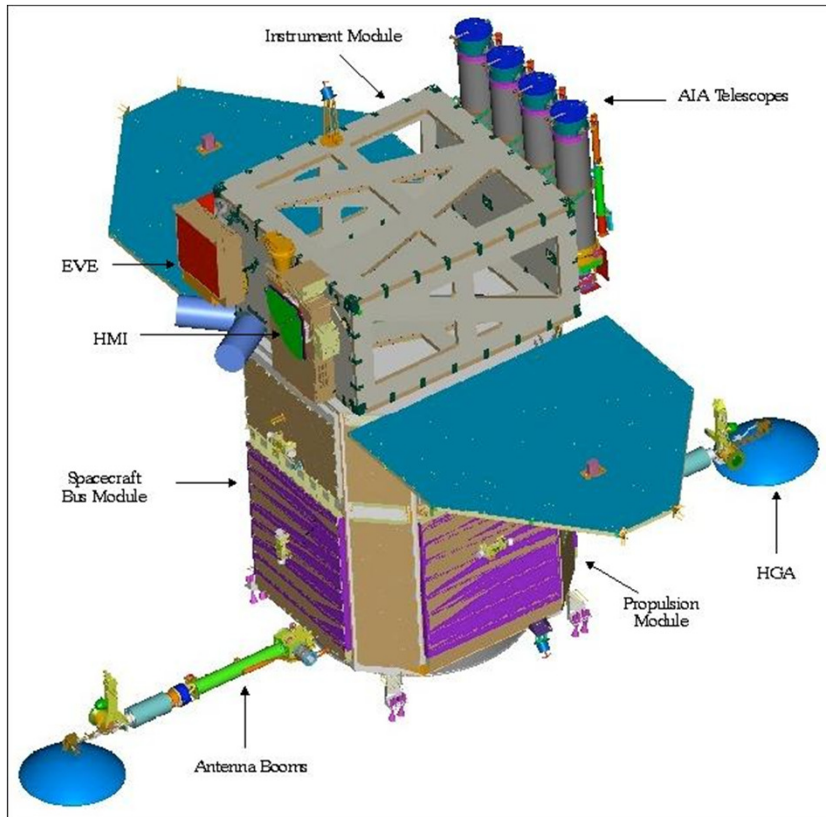
# Helioseismic and Magnetic Imager



# Helioseismic and Magnetic Imager



# Solar Dynamics Observatory

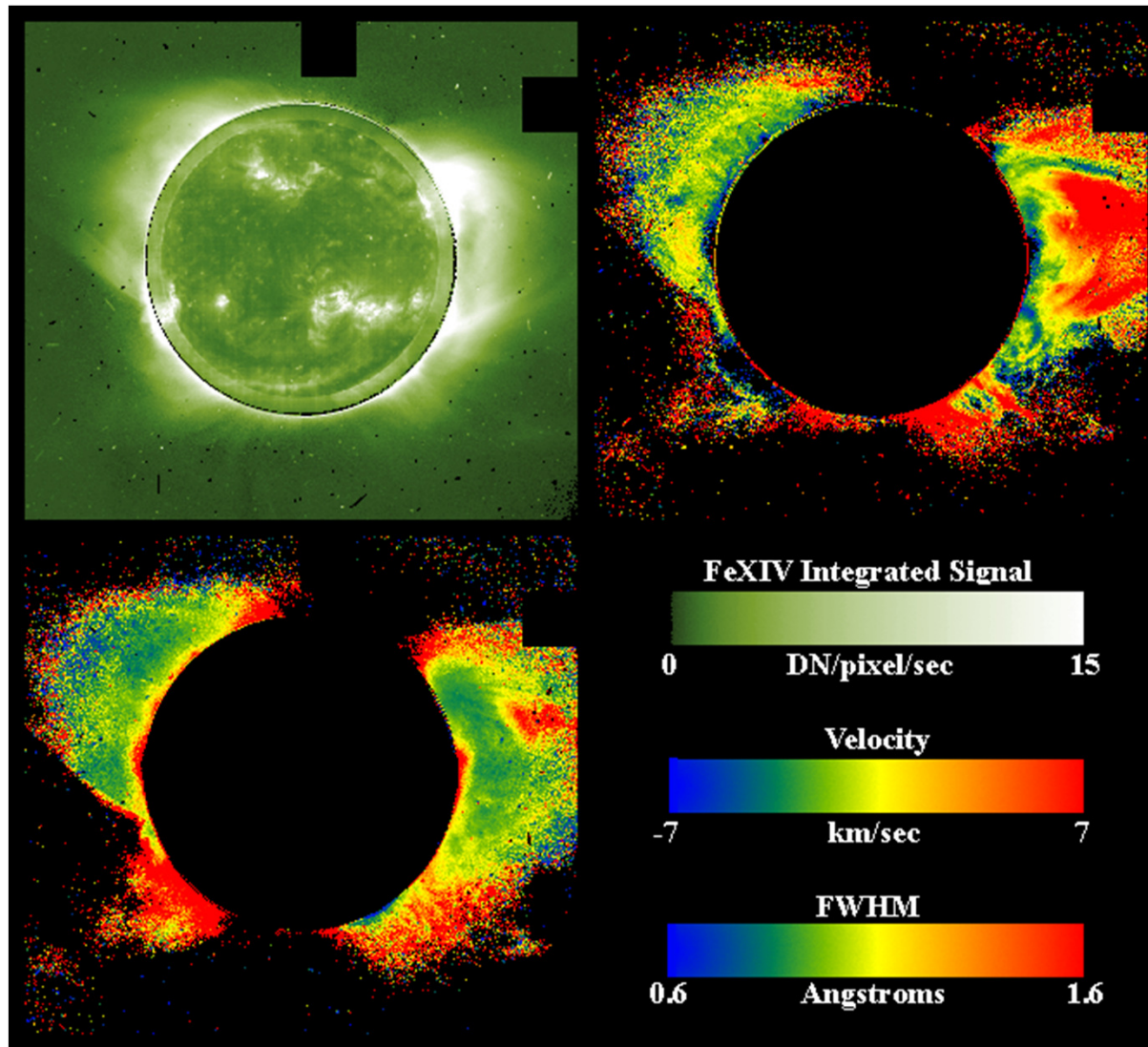


Geostationary orbit for uninterrupted observations of the Sun.



- Helioseismic and Magnetic Imager (HMI)
  - Full-disk Dopplergrams and magnetograms
- Atmospheric Imaging Assembly (AIA)
  - Full-disk images of the chromosphere and corona
- Extreme Ultraviolet Variability Experiment (EVE)
  - EUV solar irradiance

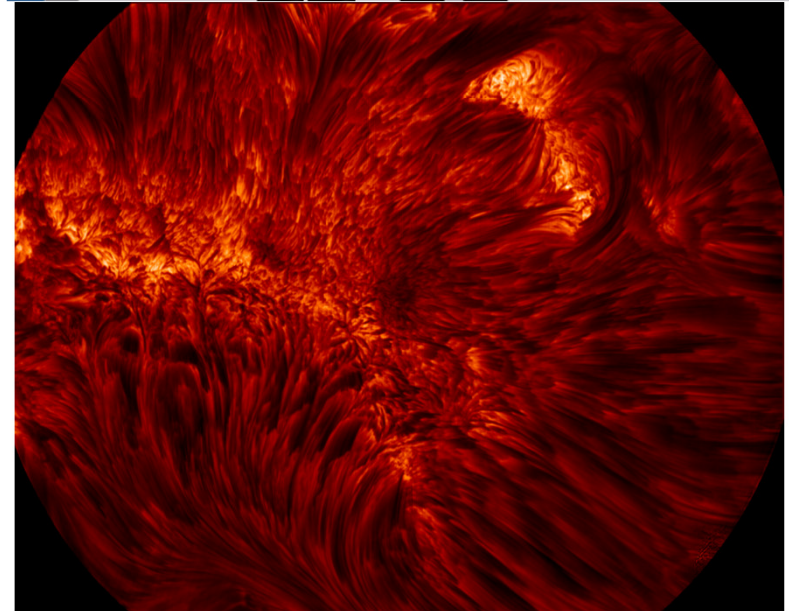
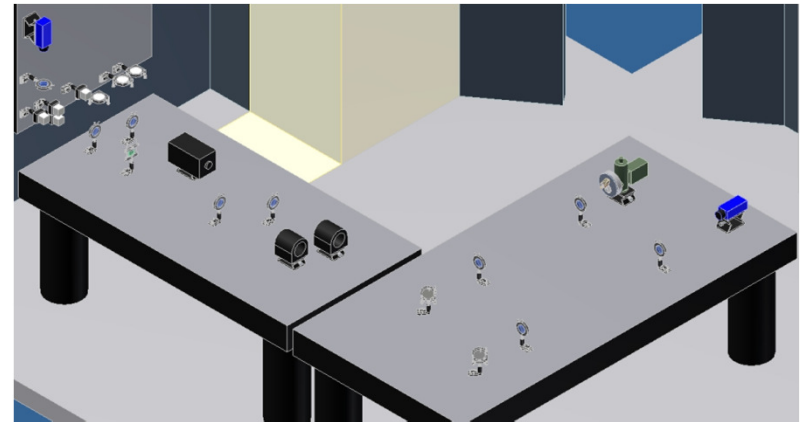
LASCO C1 coronagraph on SOHO used Fabry-Perot etalon to image the Doppler shift of coronal Fe XVI line



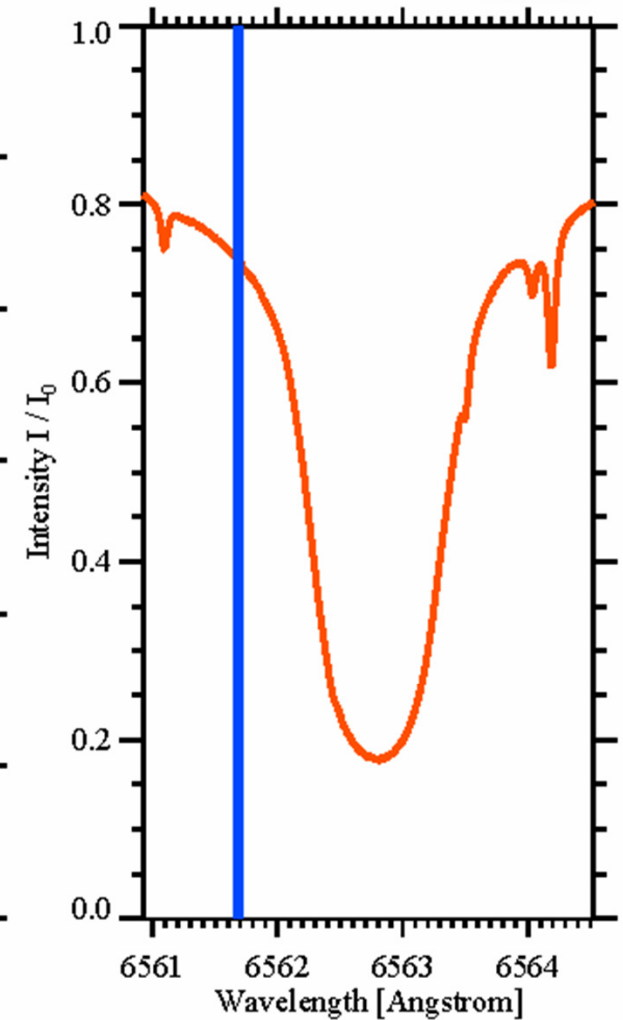
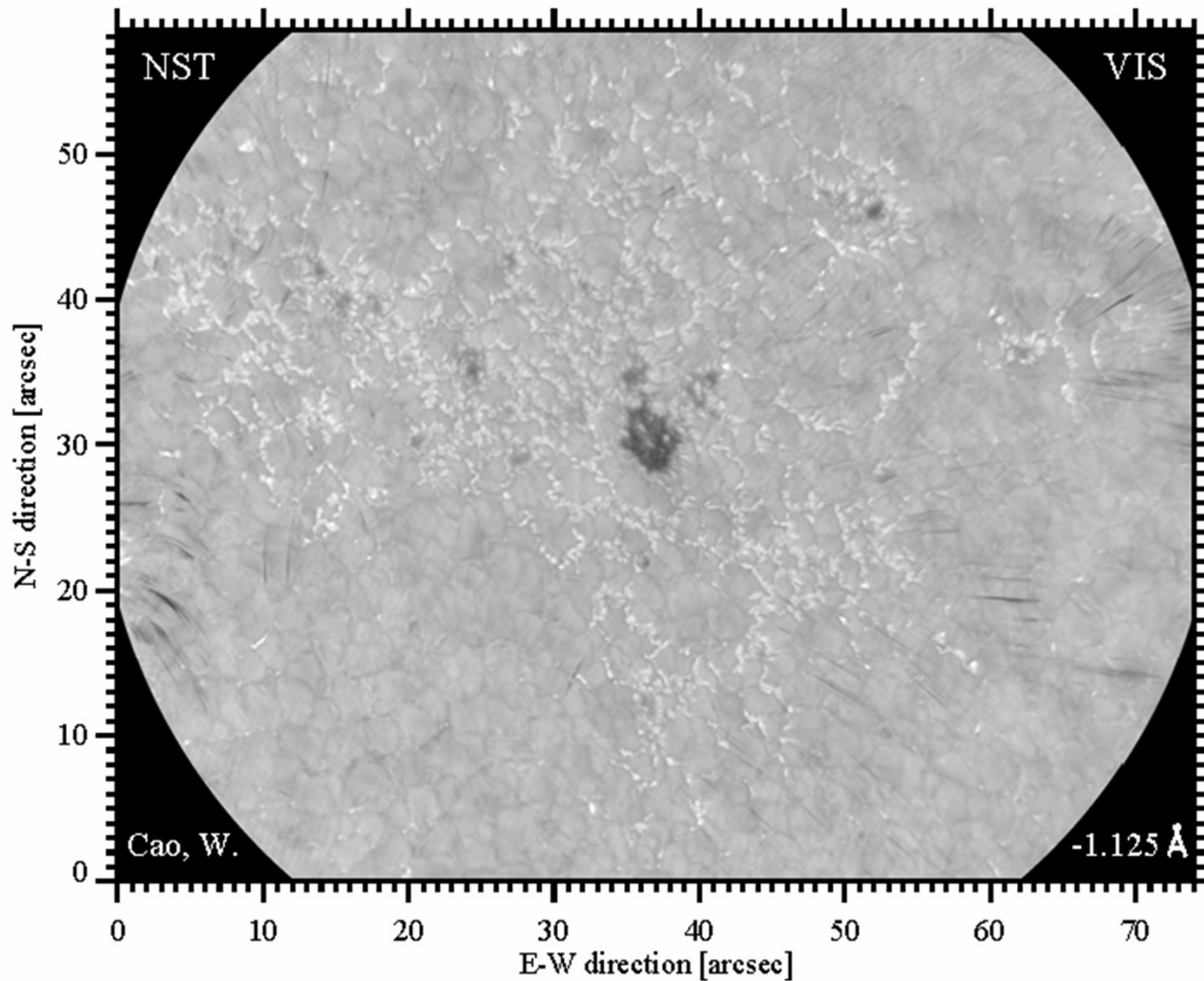
# Visible Imaging Spectrometer



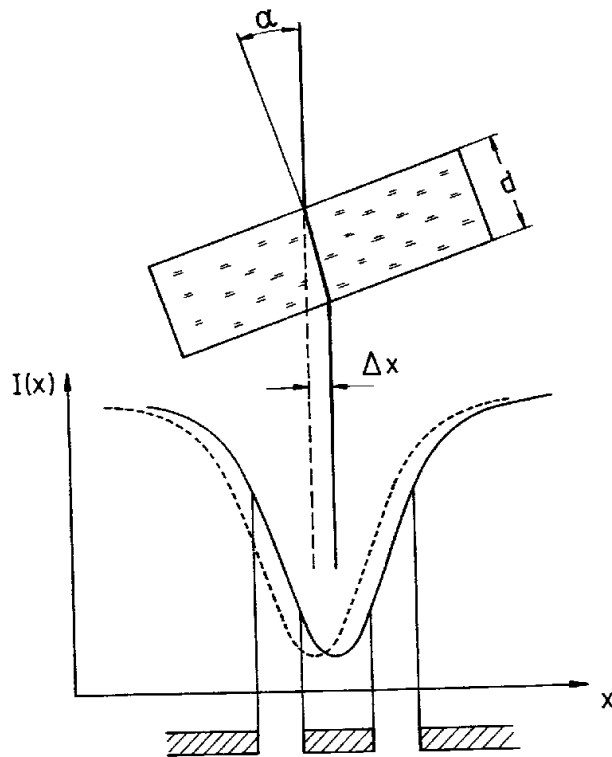
- ❖ Single Fabry-Pérot etalon ( $D = 70 \text{ mm}$ ) plus narrow band interference filter
- ❖ Wavelength coverage: 550 – 700 nm
- ❖ Band pass: 5.8 nm
- ❖ Telecentric optical configuration
- ❖ Field of view: 70" by 64"
- ❖ Available spectral lines:
  - ❖  $\text{H}\alpha$  ( $656.3 \pm 0.15 \text{ nm}$ )
  - ❖ Fe I ( $630.2 \pm 0.15 \text{ nm}$ )
  - ❖  $\text{NaD}_2$  ( $588.9 \pm 0.15 \text{ nm}$ )
  - ❖ more lines coming as needed ...
- ❖ High speed computer with SSD HDs
- ❖ Spectroscopy cadence: a 11 points scan with multi-frames selection:  $< 15 \text{ s}$



# VIS: H-alpha Observations

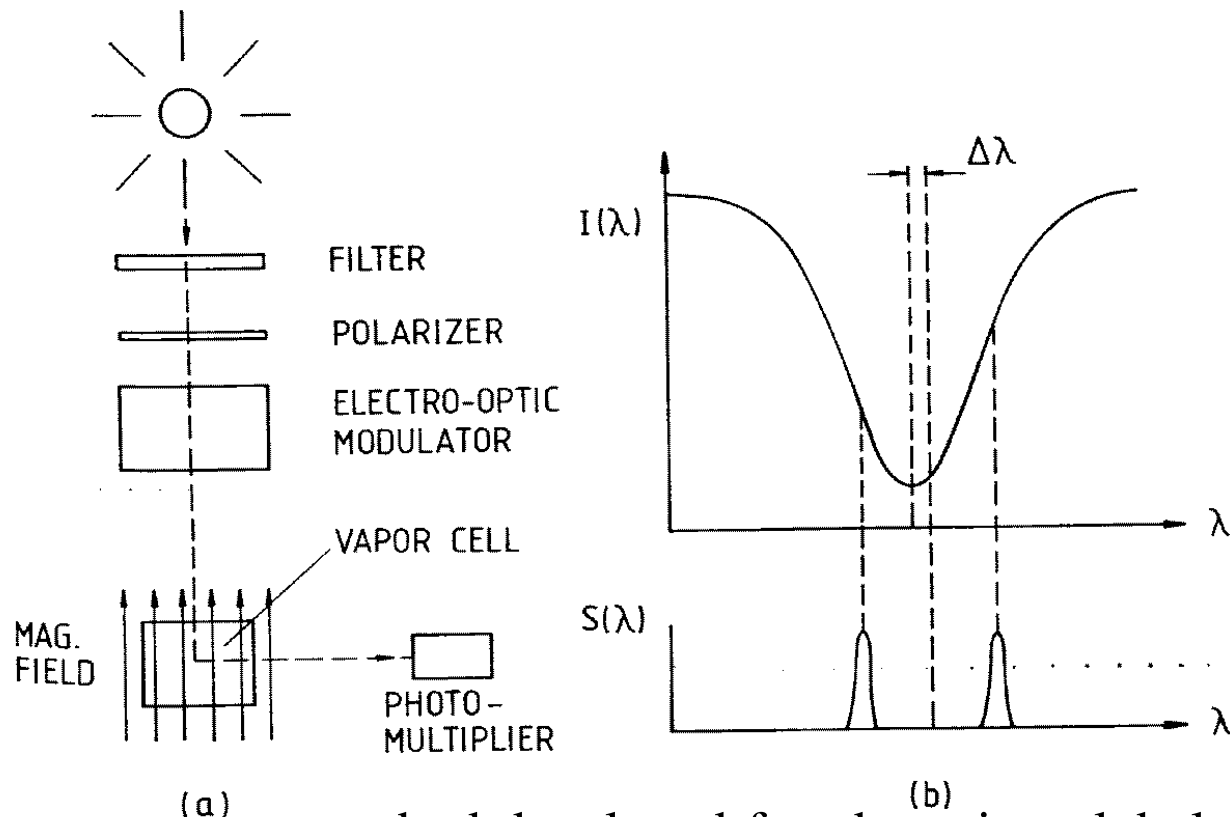


# Measurements of Line Shift. Doppler Compensator.



The Doppler compensator is a glass plate which is inclined to balance signals in the line wings recorded by two photomultipliers. It is used in magnetographs. The angle  $\alpha$  is proportional to the line shift  $\Delta\lambda_D = \lambda v/c$ . From this we can determine the line-of-sight velocity  $v$ .

# Resonance-Scattering Spectrometer.



This is a very accurate method developed for observing global oscillations of the Sun in sodium line. The vapor cell with external magnetic field provides signals of the light scattered in two wings, which are measured by a photomultiplier. The difference of these signals is proportional to the Doppler shift.

# Resonance-scattering spectrometer- GOLF instrument on SOHO (Global Oscillations at Low Frequencies)

